

**RESEARCH ARTICLE**

WILEY

Variation of pro-vasopressin processing in parvocellular and magnocellular neurons in the paraventricular nucleus of the hypothalamus: Evidence from the vasopressin-related glycopeptide copeptin

Natsuko Kawakami^{1,2,3} | Akito Otubo¹ | Sho Maejima¹ | Ashraf H. Talukder⁴ | Keita Satoh^{1,5} | Takumi Oti^{1,6} | Keiko Takanami^{1,7} | Yasumasa Ueda^{8,9} | Keiichi Itoi⁴ | John F. Morris³ | Tatsuya Sakamoto¹ | Hirotaka Sakamoto^{1,3}

¹Ushimado Marine Institute (UMI), Graduate School of Natural Science and Technology, Okayama University, Okayama, Japan

²Department of Biology, Faculty of Science, Okayama University, Okayama, Japan

³Department of Physiology, Anatomy and Genetics, University of Oxford, Oxford, UK

⁴Laboratory of Information Biology, Graduate School of Information Sciences, Tohoku University, Sendai, Miyagi, Japan

⁵Department of Anatomy, Kawasaki Medical School, Okayama, Japan

⁶Department of Biological Sciences, Faculty of Science, Kanagawa University, Hiratsuka, Kanagawa, Japan

⁷Mouse Genomics Resources Laboratory, National Institute of Genetics, Shizuoka, Japan

⁸Department of Physiology, Kyoto Prefectural University of Medicine, Kyoto, Japan

⁹Department of Physiology, Kansai Medical University, Osaka, Japan

Correspondence

Hirotaka Sakamoto, Ushimado Marine Institute (UMI), Graduate School of Natural Science and Technology, Okayama University, 130-17 Kashino, Ushimado, Setouchi, Okayama 701-4303, Japan.
Email: hsakamo@okayama-u.ac.jp

Funding information

Japan Agency for Medical Research and Development, Grant/Award Number: 961149; Japan Society for the Promotion of Science (JSPS) KAKENHI, Grant/Award Numbers: 15H05724, 15K15202, 15KK0257, 16H06280, 18K08499, 19K06475, 20K06722, 20K15837; Research Fellowships of JSPS for Young Scientists

Abstract

Arginine vasopressin (AVP) is synthesized in parvocellular- and magnocellular neuroendocrine neurons in the paraventricular nucleus (PVN) of the hypothalamus. Whereas magnocellular AVP neurons project primarily to the posterior pituitary, parvocellular AVP neurons project to the median eminence (ME) and to extrahypothalamic areas. The AVP gene encodes pre-pro-AVP that comprises the signal peptide, AVP, neurophysin (NPII), and a copeptin glycopeptide. In the present study, we used an N-terminal copeptin antiserum to examine copeptin expression in magnocellular and parvocellular neurons in the hypothalamus in the mouse, rat, and macaque monkey. Although magnocellular NPII-expressing neurons exhibited strong N-terminal copeptin immunoreactivity in all three species, a great majority (~90%) of parvocellular neurons that expressed NPII was devoid of copeptin immunoreactivity in the mouse, and in approximately half (~53%) of them in the rat, whereas in monkey hypothalamus, virtually all NPII-immunoreactive parvocellular neurons contained strong copeptin immunoreactivity. Immunoelectron microscopy in the mouse clearly showed copeptin-immunoreactivity co-localized with NPII-immunoreactivity in

Natsuko Kawakami and Akito Otubo contributed equally to this work.

This is an open access article under the terms of the Creative Commons Attribution License, which permits use, distribution and reproduction in any medium, provided the original work is properly cited.

© 2020 The Authors. *The Journal of Comparative Neurology* published by Wiley Periodicals LLC.

neurosecretory vesicles in the internal layer of the ME and posterior pituitary, but not in the external layer of the ME. Intracerebroventricular administration of a prohormone convertase inhibitor, hexa-D-arginine amide resulted in a marked reduction of copeptin-immunoreactivity in the NPII-immunoreactive magnocellular PVN neurons in the mouse, suggesting that low protease activity and incomplete processing of pro-AVP could explain the disproportionately low levels of N-terminal copeptin expression in rodent AVP (NPII)-expressing parvocellular neurons. Physiologic and phylogenetic aspects of copeptin expression among neuroendocrine neurons require further exploration.

KEYWORDS

copeptin, hypothalamo-pituitary-adrenal system, immunohistochemistry, paraventricular nucleus of the hypothalamus, processing, vasopressin, RRID: AB_2722604, RRID: AB_2061966, RRID: AB_2314234, RRID: AB_10013361, RRID: AB_2313960, RRID: AB_2722605, RRID: AB_90782

1 | INTRODUCTION

Arginine vasopressin (AVP) is a neuropeptide produced in various hypothalamic nuclei. The magnocellular neurons in the paraventricular nucleus (PVN) and the supraoptic nucleus (SON) of the hypothalamus, and small-sized neurons located in the dorsomedial portion of the suprachiasmatic nucleus (SCN), are stained intensely with antibodies against AVP or neurophysin (NP) II (Ben-Barak, Russell, Whitnall, Ozato, & Gainer, 1985; Castel & Morris, 1988; Otero-Garcia et al., 2014). Axons of AVP-producing neurons, originating from the magnocellular neurons in the PVN and the SON, traverse the internal layer of the median eminence (ME) and project to the posterior pituitary, where AVP is released into the systemic circulation from the axon terminals (Burbach, Luckman, Murphy, & Gainer, 2001). Production of AVP in the PVN and the SON, as well as its release from the posterior pituitary, is regulated by osmotic pressure and/or body fluid volume (Koshimizu et al., 2012; Murphy, Waller, Fairhall, Carter, & Robinson, 1998). AVP is also released from the dendrites of magnocellular neurons into hypothalamic neuropil, and is involved in the autocrine regulation of magnocellular neurons and paracrine regulation of other neurons in a variety of functions (Johnson & Young, 2017; Ludwig & Leng, 2006). Although SCN neurons are not part of neuroendocrine systems, AVP is also produced in the dorsomedial (shell) part of the SCN (Golombek & Rosenstein, 2010; Ramkisoensing & Meijer, 2015). Physiological roles of AVP in the SCN are still obscure, but it has been hypothesized to be involved in diverse mechanisms in the brain, which are related to the control of circadian rhythm (Gizowski, Zaelzer, & Bourque, 2016; Trudel & Bourque, 2010).

In the PVN, corticotropin-releasing factor (CRF)-producing neurons, located mainly in the anteromedial part of the nucleus, comprise a third population of neuroendocrine neurons that is capable of producing AVP (Fellmann et al., 1984; Itoi et al., 2014; Mouri et al., 1993; Whitnall, 1993). These neurons are parvocellular neurons which

project to the external layer of the ME, where CRF and AVP are released into the pituitary portal vessels from nerve endings terminating on the capillary bed (Fellmann et al., 1984). Both CRF and AVP stimulate adrenocorticotropin (ACTH) secretion from corticotrophs in the anterior pituitary, and they act synergistically in ACTH secretion when applied together to anterior pituitary cells (Fischman & Moldow, 1984; Gillies, Linton, & Lowry, 1982; Hashimoto, Murakami, Hattori, & Ota, 1984; Liu et al., 1983; Murakami, Hashimoto, & Ota, 1984; Rivier & Vale, 1983; Vale et al., 1983). The concentration of AVP in the pituitary portal vessels increases when animals are stressed (Plotsky, 1987) or have undergone adrenalectomy (Plotsky & Sawchenko, 1987). In rats, CRF and AVP are co-packaged into the same neurosecretory vesicles in the CRF- and AVP-double positive (*) subpopulation of axons in the ME, where they can be co-released from the nerve endings of the parvocellular neurons (Whitnall, Mezey, & Gainer, 1985). Therefore, both CRF and AVP are regarded as physiological secretagogues for ACTH in the pituitary (Mouri et al., 1993; Whitnall, 1993).

A fourth population of AVP-producing neurons in the PVN is located in the posterolateral part of the nucleus. These cells are categorized as parvocellular neurons, and they project to extrahypothalamic areas and to the spinal cord, and are thought to be involved in the regulation of autonomic output (Sawchenko, 1987).

The AVP gene encodes pre-pro-AVP, which is a precursor protein comprising the signal peptide, AVP, NPII, and a 39-aminoacid glycopeptide often called copeptin (Breslow, 1993; Davies, Waller, Zeng, Wells, & Murphy, 2003; Land, Schutz, Schmale, & Richter, 1982). After removal of the signal-peptide in the endoplasmic reticulum, the precursor protein is packaged into neurosecretory vesicles in the Golgi apparatus (Burbach et al., 2001; Davies et al., 2003). It is then subjected to post-translational cleavage by enzymes (prohormone convertases) and co-packaged in vesicles during its axonal transport to terminals (Hook et al., 2008). In the magnocellular neurons which project to the posterior pituitary, PC1/3, PC2, furin, and PC7 were all

strongly expressed. In the parvocellular CRF neurons, however, there was little or no expression of PC1 although PC2, furin, and PC7 were expressed there (Dong et al., 1997). At this moment, we have no knowledge of proteases in parvocellular AVP neurons that project to other regions of the brain. It is not yet clear what enzyme(s) cleaves copeptin from the NP moiety of the pre-pro-AVP, either. Copeptin constitutes the C-terminal part of the AVP precursor, and in magnocellular neurons, its cleavage from the precursor is completed at the level of posterior pituitary (Morgenthaler, Struck, Jochberger, & Dunser, 2008). Copeptin is also glycosylated, which is important for the stability of the peptide in the circulation (Bhandari et al., 2009; Blanchard et al., 2013; Bolignano et al., 2014; Wuttke et al., 2013). Activation of the AVP neurons projecting to the neurohypophysis stimulates secretion of both AVP and copeptin into systemic circulation on an equimolar basis (Morgenthaler et al., 2008). Activation of CRF/AVP neurons projecting to the ME are primarily stimulated by stress, and particular chronic stress, leading to increases in AVP expression in these neurons (de Goeij, Jezova, & Tilders, 1992; Sawchenko, Arias, & Mortrud, 1993). However, it has not been elucidated whether AVP and copeptin are released simultaneously into the portal capillaries.

Copeptin is produced as a co-product of AVP and NPII, as described above, and the AVP gene is expressed in all populations of AVP-producing neurons in the hypothalamus, i.e., the magnocellular neurons in the PVN and the SON, the parvocellular CRF neurons in the PVN, the dorsomedial group of SCN neurons, and the pre-autonomic neurons in the posterolateral part of the PVN. In the present immunofluorescence study, we used either an N-terminal copeptin antiserum or a C-terminal antiserum, together with an NPII antiserum, to examine the presence of copeptin in the hypothalamus of mice, rats, and macaque monkeys by immunofluorescence, and elucidated the co-localization of copeptin with AVP/NPII in somata of hypothalamic neuroendocrine neurons, as well as in their nerve endings in the ME. Furthermore, an immunoelectron microscopic analysis was carried out in the mouse to examine the subcellular localization of copeptin. Special attention was paid to the co-localization of copeptin with AVP/NPII within secretory vesicles. Remarkably, copeptin immunoreactivity was not uniform in different populations of AVP-producing neurons. In addition, there was a marked species difference in copeptin-immunoreactivity in the parvocellular neurosecretory neurons in the PVN.

2 | MATERIALS AND METHODS

2.1 | Animals

Adult male and female mice of the C57BL6 strain (10–12-week-old) were used in this study. For experiments probing the CRF-expressing neurons, adult male *CRF-VenusΔNeo* mice (C57BL6 strain) (Kono et al., 2017) bred in the animal facilities of Tohoku University were used. Adult male rats of the Wistar strain (10–12-week-old) were also used. Mice and rats were maintained according to the established procedure as described elsewhere (Kono et al., 2017; Sakamoto et al.,

2008). Male and female Japanese macaque monkeys, *Macaca fuscata* ($n = 2$; 2–3-year-old males, weight 2.4–2.9 kg; $n = 2$; 10–11-year-old females, weight 7.2–8.1 kg) were also used in this study. Animals were maintained in a temperature-controlled (22–24°C) room under a daily photoperiod of 12/12-hr light/dark cycle (lights on 8:00 a.m.–8:00 p.m.). These animals were shown to be free of specific pathogens. Food and water were available ad libitum. The housing and experimental protocols followed the guideline of the Ministry of Education, Culture, Sports, Science, and Technology (MEXT) of Japan, and were in accordance with the Guide for the Care and Use of Laboratory Animals prepared by Okayama University (Okayama, Japan), by Tohoku University (Miyagi, Japan), by Kyoto Prefectural University of Medicine (Kyoto, Japan), and by Kansai Medical University (Osaka, Japan). All efforts were made to minimize animal suffering and reduce the number of animals used in this study.

2.2 | Tissue preparation

Mice, rats, and monkeys were anesthetized with an overdose of sodium pentobarbital (50–90 mg/kg body weight), and transcardially perfused with physiological saline followed by 4% paraformaldehyde (PFA) (for immunohistochemistry and immunofluorescence; 17 male and four female mice; four *CRF-VenusΔNeo* adult male mice; four male rats; two male and two female Japanese macaque monkeys) or by 4% PFA + 0.1% glutaraldehyde (for electron microscopic studies; five male mice), both in 0.1 M phosphate buffer (PB, pH 7.4). Brains and neurohypophyses were immediately removed and immersed in 4% PFA in 0.1 M PB for 16–24 hr (for immunohistochemistry and immunofluorescence) at 4°C, or in 4% PFA + 0.1% glutaraldehyde in 0.1 M PB for 3 hr at room temperature (for electron microscopy). Tissues for immunofluorescence were then cryoprotected by immersion in 25% sucrose in 0.1 M PB at 4°C until they sank, then quickly frozen using powdered dry ice and cut into 30- μ m-thick coronal sections on a cryostat (CM3050 S; Leica, Nussloch, Germany). For electron microscopy, the fixed mouse brains were sectioned in the frontal plane at 200 μ m thickness with a Linear-Slicer (PRO10; Dosaka EM, Kyoto, Japan) and were immersed in 0.1 M PB.

2.3 | Immunohistochemistry and immunofluorescence

For immunohistochemistry, endogenous peroxidase activity was quenched by incubation with 1% H₂O₂ in absolute methanol for 20 min and the sections were then rinsed with PBS three times for 5 min each. These processes were omitted for immunofluorescence. After blocking nonspecific binding with 1% normal goat serum (or normal donkey serum for the goat primary antiserum) and 1% BSA in PBS containing 0.3% Triton X-100 for 30 min at room temperature, the sections were incubated with primary rabbit antiserum raised against an 8-amino acid N-terminal sequence (ATQLDGPA) of copeptin (CP8, 1:20,000 dilution) (Sato et al., 2015) (RRID:

TABLE 1 Primary antibodies used in this study

Antigen	Description	Source, host species, cat#	Working dilution	RRID
Copeptin	Synthetic peptide mapping at the N-terminal region (7–14) of mouse copeptin	Generated by our laboratory, rabbit polyclonal, CP8	1:10,000 (IF) 1:20,000 (IHC) 1:100 (EM) 1:20,000 (WB/DB)	AB_2722604
Copeptin	Synthetic peptide mapping at the C-terminus of mouse copeptin	Santa Cruz Biotechnology, goat polyclonal, sc-7812 (m-20)	1:15,000 (IF) 1:30,000 (IHC) 1:1,000 (EM) 1:30,000 (WB/DB)	AB_2061966
CRF	Human/rat CRF coupled to human α -globulins via bis-diazotized benzidine	Donated by Dr. W. Vale, rabbit polyclonal, PBL rC70	1:20,000 (IF) 1:40,000 (IHC) 1:5,000 (EM)	AB_2314234
GFP	His-GFP (full length) fusion protein	Nacalai Tesque, rat monoclonal, 04404-84	1:10,000 (IF)	AB_10013361
NPI	Soluble proteins extracted from the posterior pituitary of the rat	ATCC, mouse monoclonal, PS60, CRL-1800	1:1,000 (IF) 1:100 (EM)	AB_2722605
NPII	Soluble proteins extracted from the posterior pituitary of the rat	ATCC, mouse monoclonal, PS41, CRL-1799	1:1,000 (IF) 1:200 (EM) 1:2,000 (WB)	AB_2313960
AVP	AVP conjugated to thyroglobulin	Chemicon, rabbit polyclonal, AB1565	1:2,000 (IF) 1:4,000 (IHC)	AB_90782

Abbreviations: ATCC, American Type Culture Collection; AVP, arginine vasopressin; CRF, corticotropin-releasing factor; DB, dot blotting; EM, immunoelectron microscopy; GFP, green fluorescent protein; IF, immunofluorescence; IHC, immunohistochemistry; NPI, oxytocin-associated neurophysin I; NPII, AVP-associated neurophysin II; WB, Western blotting.

AB_2722604) or raised against C-terminus fragment of mouse copeptin (m-20, 1:30,000 dilution) (Santa Cruz Biotechnology, Dallas, TX) (RRID: AB_2061966) overnight at 4°C. Immunoreactivity was detected with a streptavidin-biotin kit (Nichirei, Tokyo, Japan), followed by DAB development according to our previously reported method (Sakamoto et al., 2008).

To demonstrate co-expression of copeptin or CRF in AVP neurons, double-immunofluorescence staining for copeptin (1:10,000 dilution), AVP (1:2,000 dilution), or CRF (1: 20,000 dilution) and AVP-NPII (1:1,000 dilution), or oxytocin-NPI (1:1,000 dilution) was performed. A rabbit polyclonal antiserum for AVP (Chemicon, Temecula, CA) (RRID: AB_90782) was used. Mouse monoclonal antibodies for NPII (PS41; RRID: AB_2313960) and NPI (PS60; RRID: AB_2722605) were used, and have previously been shown to be specific for AVP and oxytocin neurons, respectively (Castel, Morris, Whitnall, & Sivan, 1986; Wang, Ward, & Morris, 1995). The rabbit polyclonal antiserum against rat CRF (PBL rC70; RRID: AB_2314234), which was kindly donated by Wylie Vale, has been characterized elsewhere (Sawchenko, Swanson, & Vale, 1984). Specific staining for AVP and CRF were abolished by pre-adsorption of the antisera for 1 hr at room temperature with 50 μ g/ml synthetic AVP or mouse CRF before use. We further confirmed by Western blot analysis the specificity for the NPII antibody. The monoclonal antibody (PS41) labeled a single band at approximately the expected molecular weight of ~11 kDa on the blots of mouse, rat, and macaque monkey posterior pituitary. Western blot analysis also showed the specificity for the NPI antibody (PS60) in the mouse posterior pituitary. A goat polyclonal

antiserum for copeptin (m-20) raised against an oligopeptide near the C-terminus of copeptin of mouse origin at a dilution of 1:15,000 was also used as described previously (Itoi et al., 2014). Control procedures for the DAB method were performed using pre-absorption of the working dilution (CP-8; 1:20,000 or m-20; 1:30,000) of the primary antiserum with a saturating concentration of the antigen (50 μ g/ml; N-terminus fragment of mouse copeptin₇₋₁₄ [ATQLDGPA] or C-terminus fragment of mouse copeptin₂₀₋₃₉ [RLVQLAGTRESVDSAKPRVY]) for 1 hr at room temperature before use. Immunostained sections were observed under the Olympus FSX100 microscope (Tokyo, Japan).

To detect the Venus signals in tissues from *CRF-Venus Δ Neo* mice, we performed immunofluorescence for detection of green fluorescent protein (GFP) to intensify the Venus signal (for localizing CRF neurons) as described previously (Kono et al., 2017). Primary rat monoclonal anti-GFP antibody (1:10,000 dilution) (Nacalai Tesque, Kyoto, Japan; RRID: AB_10013361) was used. Double immunofluorescence for GFP and NPII or copeptin was performed as described above. Alexa Fluor 546-linked anti-mouse IgG (Molecular Probes, Eugene, OR), Alexa Fluor 488-linked anti-goat IgG (Molecular Probes), Alexa Fluor 488-linked anti-rat IgG (Molecular Probes), and Alexa Fluor 488-linked anti-rabbit IgG (Molecular Probes) were used for detection at a dilution of 1:1,000. Images of immunostained sections were captured by confocal laser scanning microscopy (FluoView 1000, Olympus). The antibodies used in this study are showed in Table 1.

The data are presented as the mean \pm SEM and were analyzed using Statcel4 software. Statistical analyses of the proportion of copeptin-negative ($\bar{\square}$) /NPII⁺ neurons were performed using one-way

analysis of variance (ANOVA) (in male mice or rats) or two-way ANOVA (sex difference and right/left difference in mice). When significance was found using ANOVA, the post hoc Bonferroni/Dunn test was performed.

2.4 | Post-embedding immunoelectron microscopy

Preparations were dehydrated through increasing concentrations of methanol, embedded in LR Gold resin (Electron Microscopy Sciences, PA), and polymerized under ultraviolet lamps at -20°C for 24 hr. Ultrathin sections (70 nm in thickness) were collected on nickel grids coated with a Collodion film (or without for triple labeling), rinsed with PBS several times, then incubated with 2% normal goat serum and 2% BSA in 50 mM Tris(hydroxymethyl)-aminomethane-buffered saline (TBS; pH 8.2) for 30 min to block nonspecific binding. The sections were then incubated with the rabbit polyclonal antiserum against N-terminal copeptin (CP8, 1:100 dilution), or the goat polyclonal antiserum against C-terminal copeptin (m-20, 1:1,000 dilution), and the PS41 mouse monoclonal antibody against NPII (1:200 dilution) (Castel et al., 1986) for 2 hr at room temperature. The rabbit polyclonal antiserum against rat CRF was also used at 1:5,000 for 2 hr at room temperature. For double immunoelectron microscopy, after incubation with the primary antibodies, the sections were washed with PBS, then incubated with a goat antibody against rabbit IgG conjugated to 10 nm gold particles (1:50 dilution) (BBI Solutions, Cardiff, UK) and/or a goat antibody against mouse IgG conjugated to 15 nm gold particles (1:50 dilution) (BBI Solutions) for 1 hr at room temperature.

Triple immunoelectron microscopy with antibodies for AVP-associated NPII, oxytocin-associated NPI, and copeptin was performed using the front and back of ultrathin sections mounted on nickel grids. First, immunocytochemistry with 2 primary antibodies (anti-NPII; PS41 and copeptin) was performed on one side of the section and detected using 15 and 10 nm colloidal gold particles. Next, the other antibody (anti-NPI; PS60) was detected using 5 nm colloidal gold particles on the other side of the section. Finally, the sections were contrasted with uranyl acetate and lead citrate and viewed using an H-7650 (Hitachi, Tokyo, Japan) or JEM-1010 (JEOL, Tokyo, Japan) electron microscope operated at 80 kV. The antibodies used in this study are shown in Table 1.

2.5 | Intracerebroventricular injection of a prohormone convertase inhibitor, hexa-D-arginine amide

Adult male mice were anesthetized with an intraperitoneal injection of medetomidine hydrochloride (0.3 mg/kg body weight), midazolam (4 mg/kg body weight), and butorphanol tartrate (5 mg/kg body weight) and then placed in the stereotaxic apparatus for the intracerebroventricular injection of the protease inhibitor (furin inhibitor II) (hexa-D-arginine amide [D6R]) (Sigma, St. Louis, MO) dissolved in PBS.

The needle of a syringe (701 RN) (Hamilton, Reno, NV) filled with D6R was inserted into the right lateral ventricle (location of the needle tip: -0.4 mm caudal to the bregma, -1.0 mm lateral to the midline, 2.0 mm below the dura). After inserting the needle, D6R ($9\ \mu\text{g}$ in $2\ \mu\text{l}$ PBS) was infused into the lateral ventricle at a flow rate of $1\ \mu\text{l}/\text{min}$ ($n = 6$). Control mice were infused with the same volume of PBS ($n = 4$). Mice were perfused with fixative 18 hr after D6R or PBS injection, and then brains were removed. Double immunofluorescence for NPII and copeptin was then performed as described above.

2.6 | Western blotting

Adult male mice were sacrificed by decapitation to obtain the fresh brains. Brains were cut into $400\ \mu\text{m}$ thick coronal sections using a vibrating microtome (7000smz-2; Campden Instruments). For each mouse, a section containing the SON (Bregma -0.58 to -0.94 mm) region determined based on the Mouse Brain in Stereotaxic Coordinates (Franklin & Paxinos, 2007) was mounted on glass, and the SON was dissected bilaterally by use of a stainless needle (outer diameter 1.20 mm, inner diameter 0.94 mm). The samples (1/5 SON protein/lane and 1/50 posterior pituitary protein/lane) were boiled in $10\ \mu\text{l}$ sample buffer containing 62.5 mM tris(hydroxymethyl)-aminomethane-HCl (Tris-HCl; pH 6.8), 2% SDS, 25% glycerol, 10% 2-mercaptoethanol, and a small amount of bromophenol blue. Samples were run on a 4–20% SDS-PAGE and electroblotted onto a polyvinylidene difluoride (PVDF) membrane (Bio-Rad Laboratories, Hercules, CA) using a semidry blotting apparatus (Bio-Rad Laboratories). Membranes were blocked with PVDF Blocking Reagent for Can Get Signal (TOYOBO, Tokyo, Japan) for 30 min at room temperature and incubated for 1 hr at room temperature in Can Get Signal Solution 1 (TOYOBO) with our custom N-terminal copeptin antiserum (CP8, 1:20,000 dilution), with the antiserum raised against the C-terminus of mouse copeptin (m-20, 1:30,000 dilution), or with the NPII antibody (PS41, 1:2,000 dilution). Blotted membranes were washed three times with 0.05% Tween 20 in Tris-HCl-buffered saline (TBST) and incubated with horseradish peroxidase-conjugated goat polyclonal antibody against rabbit IgG (Bio-Rad Laboratories) at 1:10,000 dilution, with horseradish peroxidase-conjugated rabbit polyclonal antibody against goat IgG (Bio-Rad Laboratories) at 1:10,000 dilution, or with horseradish peroxidase-conjugated goat polyclonal antibody against mouse IgG (Bio-Rad Laboratories) at 1:10,000 dilution in Can Get Signal Solution 2 (TOYOBO) for 1 hr at room temperature. After washing for three times with TBST, blots were visualized by Immuno-Star WesternC Chemiluminescence Kit (Bio-Rad Laboratories). Images of the different immunoblots were slightly adjusted in brightness and contrast to provide a uniform background.

Dot blot analysis was further performed with our custom N-terminal copeptin antiserum (CP8) and the antiserum raised against the C-terminus of mouse copeptin (m-20). Each antigen of the mouse origin: copeptin_{7–14} peptide (ATQLDGPA) and copeptin_{20–39} (RLVQLAGTRESVDSAKPRVY) were blotted onto the PVDF membrane. The blotted membrane was immunostained as described above.

3 | RESULTS

3.1 | Species difference in copeptin expression in parvocellular neurosecretory neurons in the PVN

Figure 1 shows the amino acid sequences of copeptin in seven mammals including the mouse, rat, and monkey. The epitope against which the CP8 antiserum was raised is indicated by asterisks above the sequences. This region is well conserved across mammals (stars below the sequences) and is identical in the mouse, the rat, the monkey, and the human. The specificity of our custom N-terminal CP8 copeptin antiserum was confirmed by an absorption experiment in which the primary rabbit antiserum against mouse copeptin₇₋₁₄ was preabsorbed with an excess amount of mouse copeptin₇₋₁₄ (ATQLDGPA), whereas the staining was not affected by treatment with the same concentration of synthetic C-terminus fragment of mouse copeptin₂₀₋₃₉ (RLVQLAGTRESVDSAKPRVY) (Figure 2). Unless otherwise stated the antiserum is the N-terminal CP8 antiserum. AVP neurons were immunoidentified with the anti-NPll antibody that has been well characterized and used as a marker for AVP neurons (Ben-Barak et al., 1985; Castel & Morris, 1988). Because the localization of AVP- and NPll-expressing neurons is identical in the rodent brain (Figures 3 and 4), NPll-immunofluorescence was used as a marker for AVP neurons in this study.

In the mouse, most magnocellular NPll⁺ cells also exhibit copeptin-immunoreactivity in both the PVN and the SON. In the PVN, however, a major proportion (~87%) of NPll⁺ neurons in the medial subgroup (PaMP) of parvocellular neurons did not contain immunodetectable copeptin (Figure 5; arrowheads) (Table 2). These copeptin⁻/NPll⁺ neurons were most prominent in the anterior parvocellular part (PaAP) (~94%) and the posterior parvocellular part (PaPo) (~93%) of the PVN (Figure 5; arrowheads) (Table 2). A preliminary investigation of various groups of parvocellular neurons (medial, anterior, and posterior [lateral] groups in mice) revealed no obvious

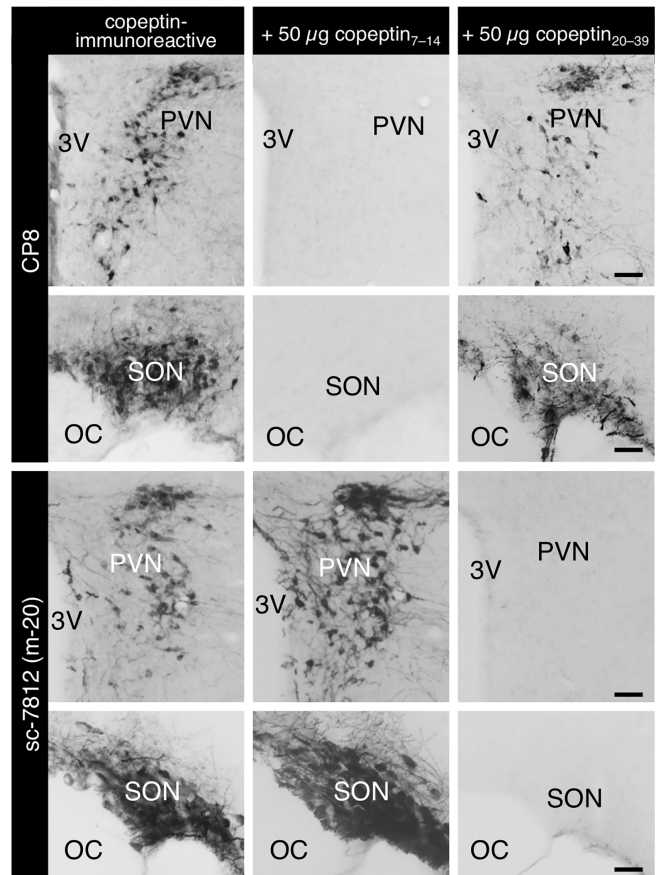


FIGURE 2 Immunohistochemical analysis of copeptin in the adult mouse paraventricular (PVN) and supraoptic (SON) nuclei. Immunoreactivity against copeptin was mainly observed in magnocellular neurons of the PVN and SON. Controls in which copeptin antiserum preabsorbed with a saturating concentration of the antigen (50 µg/ml) for 1 hr at room temperature before use was substituted for the anti-copeptin antiserum showed a complete absence of copeptin-like immunoreactivities in the PVN and SON. Scale bars, 200 µm. OC, optic chiasm; 3V, third ventricle

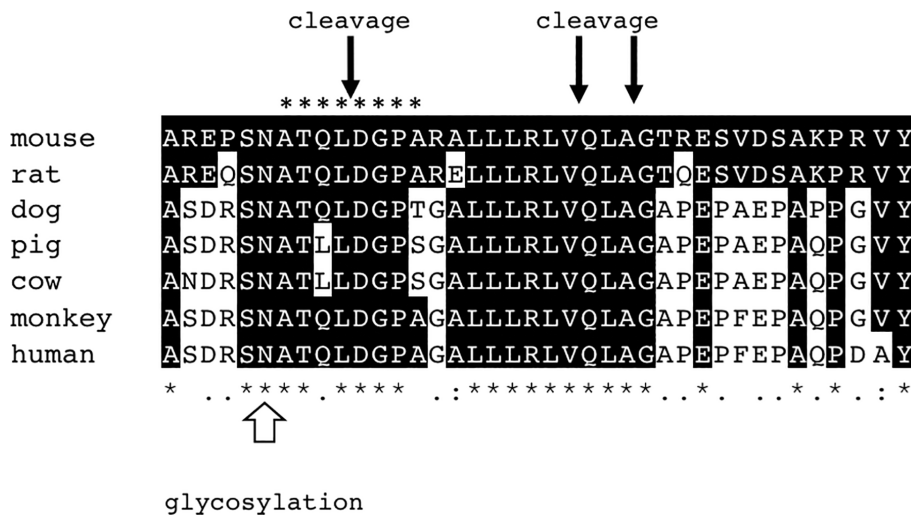


FIGURE 1 A comparison of the amino acid sequences of copeptin in seven mammals including the mouse, the rat, and the macaque monkey. Residue identity to mouse copeptin is denoted by highlight. The antigen epitope site is highlighted by asterisks above the sequences (ATQLDGPA). The white arrow indicates a possible glycosylation site. The black arrows indicate three possible cleavage sites. Amino acids identical to those in other species are indicated by stars (*). Colon (:) indicates conserved substitution and period (.) indicates semiconserved substitution

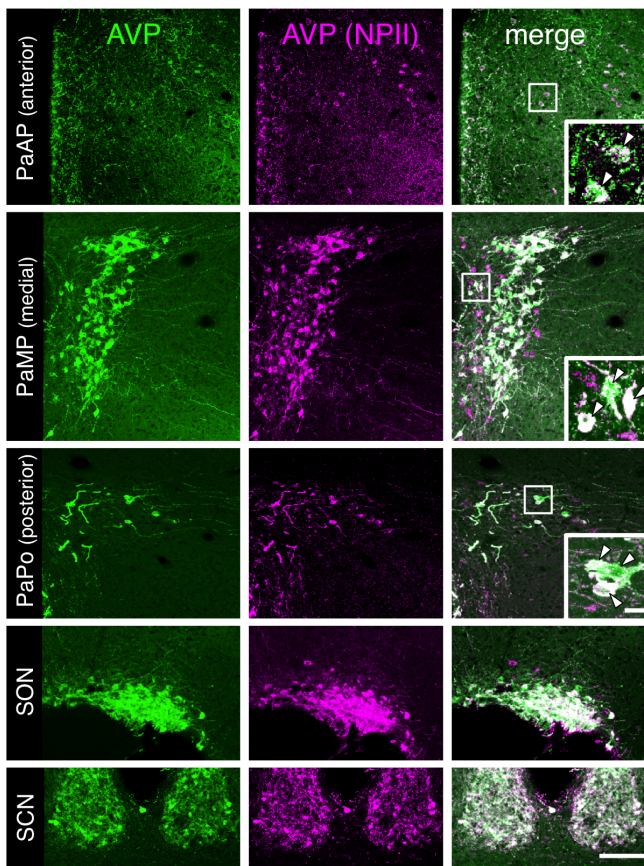


FIGURE 3 Double-label immunofluorescence for vasopressin (AVP) and AVP-neurophysin (NPII) in the paraventricular (PVN) and supraoptic (SON) nuclei, or in the suprachiasmatic nucleus (SCN) in the mouse. Immunoreactivities against AVP (green) and NPII (magenta) were merged in each right *panel* (overlap white), respectively. The outlined areas in merged images are enlarged at the bottom right of the figure. *Scale bars*, 100 μm , and 10 μm in enlarged images. PaAP, anterior parvocellular part of the PVN; PaMP, medial parvocellular part of the PVN; PaPo, the posterior part of the PVN [Color figure can be viewed at wileyonlinelibrary.com]

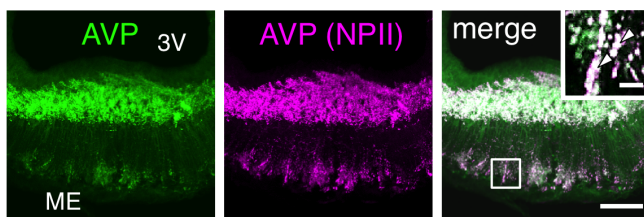


FIGURE 4 Double-label immunofluorescence for vasopressin (AVP) and AVP-neurophysin (NPII) in the mouse median eminence (ME). Immunoreactivities against AVP (green) and NPII (magenta) were merged in each right *panel* (overlap white), respectively. The outlined fibers doubly immunopositive for AVP and NPII. *Scale bars*, 50 μm , and 5 μm in the enlarged image. 3V, third ventricle [Color figure can be viewed at wileyonlinelibrary.com]

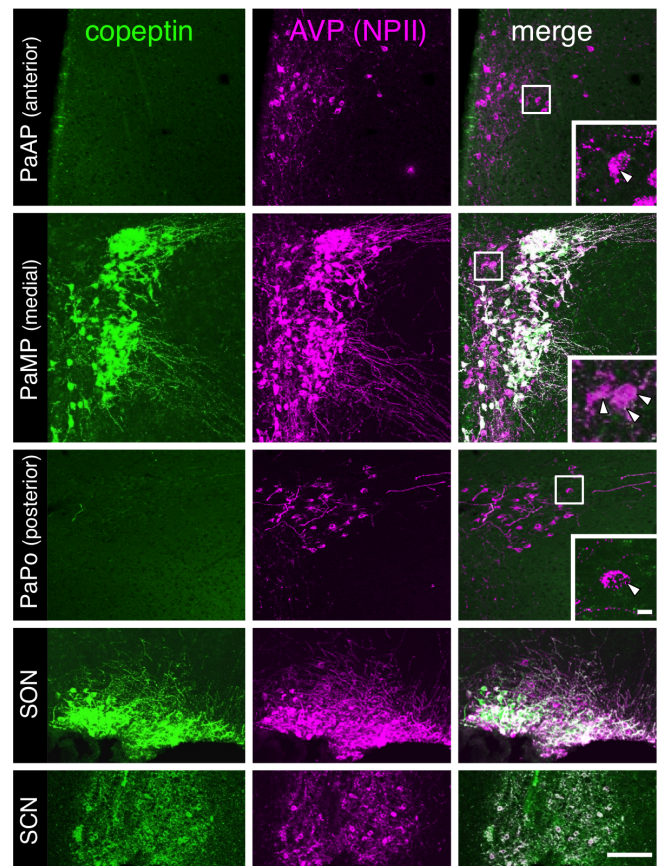


FIGURE 5 Double-label immunofluorescence for N-terminal copeptin and vasopressin (AVP)-neurophysin (NPII) in the paraventricular (PVN) and supraoptic (SON) nuclei, and in the suprachiasmatic nucleus (SCN) in the mouse. Immunoreactivity against copeptin (green) and AVP (NPII) (magenta) was merged in each right *panel* (overlap white), respectively. The outlined areas in merged images are enlarged at the bottom right of the figure. *Arrowheads* indicate AVP (NPII)-immunoreactive parvocellular PVN neurons that did not express immunodetectable amounts of copeptin. *Scale bars*, 100 μm , and 10 μm in enlarged images. PaAP, anterior parvocellular part of the PVN; PaMP, medial parvocellular part of the PVN; PaPo, the posterior part of the PVN [Color figure can be viewed at wileyonlinelibrary.com]

differences and was complicated by the lack of an obvious size difference between magnocellular and parvocellular AVP neurons. No sex difference or right/left difference was observed in the ratio of copeptin⁻/NPII⁺ neurons in the parvocellular PVN of mice (Table 3). In contrast to the parvocellular PVN neurons, almost all NPII⁺ neurons in the SCN (a nucleus that contains small-sized AVP neurons) did exhibit copeptin-immunoreactivity (Figure 5). As expected, oxytocin neurons identified by NPI immunoreactivity did not exhibit copeptin-immunoreactivity in either the PVN or SON (Figure 6). Similar results were obtained in the rat (Figure 7), but the proportion of copeptin⁻/NPII⁺ neurons in the parvocellular PVN was less marked (~53%) compared with that in the mouse (Table 2). In the macaque monkey, remarkably, virtually all NPII⁺ neurons in both the magnocellular and

	Number of males	PaAP	PaMP	PaV	PaPo	Total
Mouse	5	94.0 ± 0.5*	87.3 ± 1.1	84.8 ± 0.3	93.2 ± 0.3*	89.6 ± 0.3 (n = 4,461)
Rat	4	60.2 ± 2.7	62.5 ± 4.1	55.1 ± 5.1	20.5 ± 4.5†	53.1 ± 1.7 (n = 2,941)

Abbreviations: NP, neurophysin; PaAP, anterior parvocellular part of the PVN; PaMP, medial parvocellular part of the PVN; PaV, the ventral part of the PVN; PaPo, the posterior part of the PVN; PVN, paraventricular nucleus.

* $p < .01$, versus PaMP and PaV.

† $p < .01$, versus PaAP, PaMP, and PaV.

	Number of animals	Left	Right	Total
Male	5	89.1 ± 0.5	90.1 ± 0.9	89.6 ± 0.3 (n = 4,461)
Female	4	89.1 ± 0.4	89.0 ± 0.2	89.1 ± 0.2 (n = 3,580)

Abbreviations: NP, neurophysin; PVN, paraventricular nucleus.

TABLE 2 Proportion (%) of N-terminal-copeptin-negative/vasopressin-associated NP II-positive neurons in the mouse and rat parvocellular PVN of the hypothalamus in males

TABLE 3 Proportion (%) of N-terminal-copeptin-negative/vasopressin-associated NP II-positive neurons in the parvocellular of the hypothalamus in mice

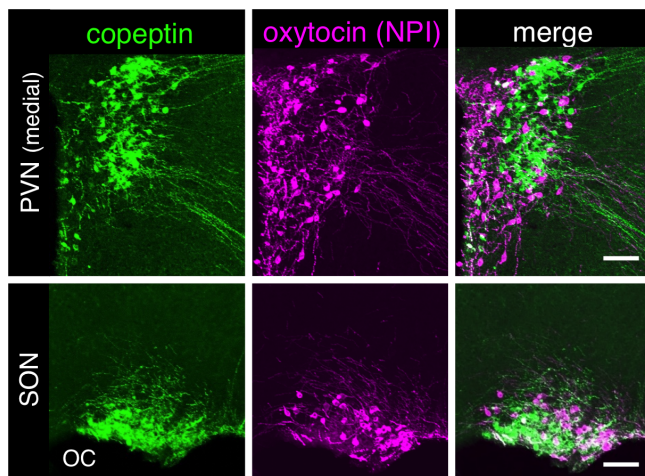


FIGURE 6 Double-label immunofluorescence for copeptin and oxytocin-neurophysin (NPI) in the mouse paraventricular (PVN) (middle part) and supraoptic (SON) nuclei. Immunoreactivities against copeptin (green) and NPI (magenta) were merged in each right panel, respectively. Scale bars, 100 μ m. OC, optic chiasma; 3V, third ventricle [Color figure can be viewed at wileyonlinelibrary.com]

parvocellular division were also copeptin-immunoreactive (Figure 8). No obvious sex difference was observed in monkeys in terms of copeptin- and NP II-immunoreactivity.

In the internal layer of the ME that contains axons of magnocellular neurons originating from the PVN or SON and projecting to the posterior pituitary, virtually all NP II⁺ fibers exhibited copeptin-immunoreactivity in the mouse, rat, and monkey (Figure 9a). However, in the external layer of the mouse ME, where the parvocellular CRF axons terminate, copeptin immunoreactivity could be detected in only a small number of NP II⁺ fibers (Figure 9a; arrowheads). In the external layer of the rat ME, co-expression of

NP II- and copeptin-immunoreactivity was observed more frequently in the external layer of the ME than in the mouse, but less frequently than in the monkey (Figure 9b; arrowheads). In the macaque monkey, most NP II⁺ fibers were copeptin-immunoreactive in both the internal and external layer of the ME (Figure 9c; arrowheads).

3.2 | Expression of NP II or copeptin in parvocellular CRF neurons in mice

Expression of NP II and CP8-detectable copeptin in the parvocellular CRF neurons was examined in the CRF-Venus Δ Neo mouse. In the parvocellular PVN, very few (one or two cells per section) Venus⁺ neurons showed NP II-immunoreactivity (Figure 10a; arrowheads) or copeptin-immunoreactivity (Figure 10b; arrowheads). We next studied co-localization of CRF with NP II in the ME of a wild-type mouse. CRF-immunoreactive fibers were detectable only in the external layer of the ME, and approximately half of the CRF-immunoreactive fibers contained NP II-immunoreactivity (Figure 10c; arrowheads). NP II⁺ fibers were intensively stained in the internal layer of the mouse ME of the wild-type mouse, but were devoid of CRF-immunoreactivity (Figure 10c). However, NP I⁺ fibers were hardly observed in the external layer of the ME in the mouse (Figure 11).

Preliminary experiments using a copeptin m-20 antiserum raised against an epitope near the C-terminus of mouse copeptin₂₀₋₃₉ revealed copeptin-immunoreactivity in virtually all NP II-expressing magnocellular and parvocellular neurons in the mouse PVN (Figure 12). The specificity of the Santa Cruz copeptin antiserum (m-20) was confirmed by an absorption experiment in which the primary goat antiserum against the C-terminus of mouse copeptin was preabsorbed with an excess amount of synthetic C-terminus fragment of mouse copeptin₂₀₋₃₉ (RLVQLAGTRESVDSAKPRVY), whereas the staining was not affected by treatment with the same concentration of mouse N-terminus fragment of mouse copeptin₇₋₁₄ (ATQLDGPA) (Figure 2).

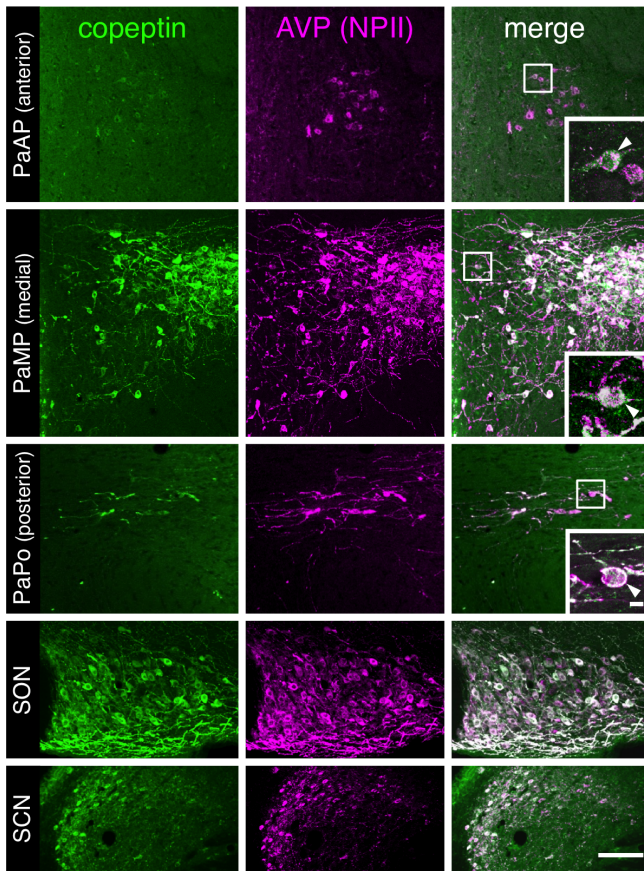


FIGURE 7 Double-label immunofluorescence for N-terminal copeptin and vasopressin (AVP)-neurophysin (NPII) in the paraventricular (PVN) and supraoptic (SON) nuclei, and in the suprachiasmatic nucleus (SCN) in the rat. Immunoreactivity against copeptin (green) and AVP (NPII) (magenta) was merged in each right *panel* (overlap white), respectively. The outlined areas in merged images are enlarged at the bottom right of the figure. *Arrowheads* indicate AVP (NPII)-immunoreactive parvocellular PVN neurons that did not (or very weakly) express immunodetectable amounts of copeptin. *Scale bars*, 100 μm , and 10 μm in enlarged images. PaAP, anterior parvocellular part of the PVN; PaMP, medial parvocellular part of the PVN; PaPo, the posterior part of the PVN [Color figure can be viewed at wileyonlinelibrary.com]

3.3 | Co-localization of copeptin with NPII within secretory vesicles in mice

Triple immunoelectron microscopy was carried out to examine co-localization of NPII, NPI, and CP8-detectable copeptin within neurosecretory vesicles in the mouse. Both NPII and copeptin were detected within axons of neurosecretory neurons in the posterior pituitary, where they were co-associated within neurosecretory vesicles (Figure 13a,b). NPI was also detected in axon terminals, but no copeptin-immunoreactivity was observed in NPI-labeled terminals adjacent to NPII-labeled terminals (Figure 13c). Numerous neurosecretory vesicles located in cell bodies and dendrites of magnocellular neurons in the SON were immunolabeled for both copeptin and NPII (Figure 14a–c). However, copeptin-immunoreactivity was not

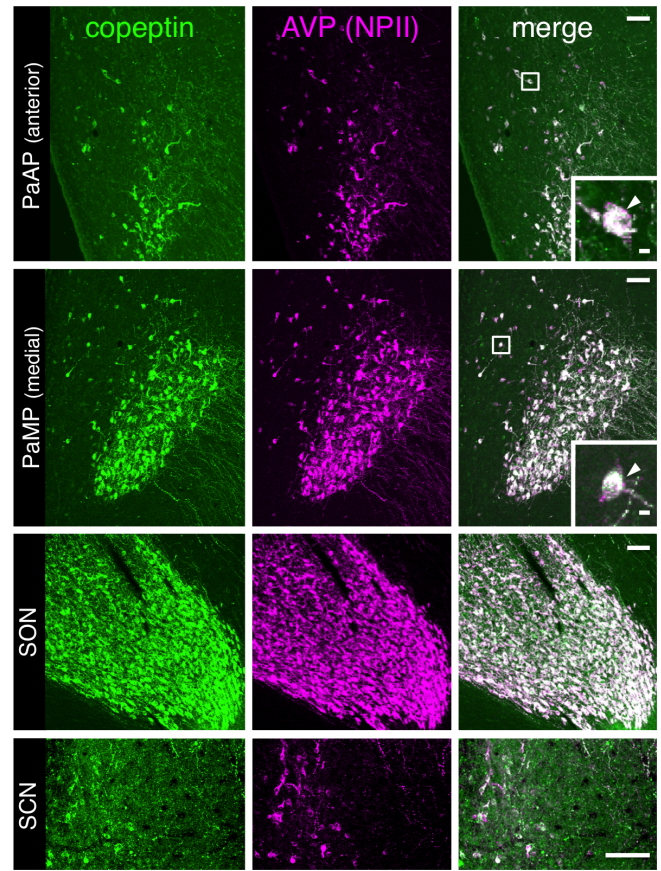


FIGURE 8 Double-label immunofluorescence for N-terminal copeptin and vasopressin (AVP)-neurophysin (NPII) in the paraventricular (PVN) and supraoptic (SON) nuclei, and in the suprachiasmatic nucleus (SCN) in the macaque monkey. Immunoreactivity against copeptin (green) and AVP (NPII) (magenta) was merged in each right *panel* (overlap white), respectively. The outlined areas in merged images are enlarged at the bottom right of the figure. Virtually all NPII⁺ neurons in both the magnocellular and parvocellular division were also copeptin-immunoreactive (*arrowheads*). *Scale bars*, 100 μm , and 10 μm in enlarged images. PaAP, anterior parvocellular part of the PVN; PaMP, medial parvocellular part of the PVN [Color figure can be viewed at wileyonlinelibrary.com]

observed in immature neurosecretory vesicle cores within the Golgi apparatus (Figure 15). In magnocellular neurons in the PVN, many neurosecretory vesicles were labeled for both copeptin and NPII and the vesicles were ~ 160 nm in diameter (Figure 16a). The size was similar to that of neurosecretory vesicles in the SON (Figures 14–16). In parvocellular PVN neurons, there were also numerous dense-cored neurosecretory vesicles (~ 100 nm in diameter) that contained NPII-immunoreactivity, but these vesicles were devoid of copeptin-immunoreactivity (Figure 16b; *arrows*).

Next, we examined co-localization of NPII and copeptin in the mouse ME. The two layers of the ME, that is, the internal and external layers, investigated in the present immunoelectron microscopy, are shown schematically in Figure 17a. In the internal layer of the ME, immunoreactivity for both NPII and copeptin was intense in

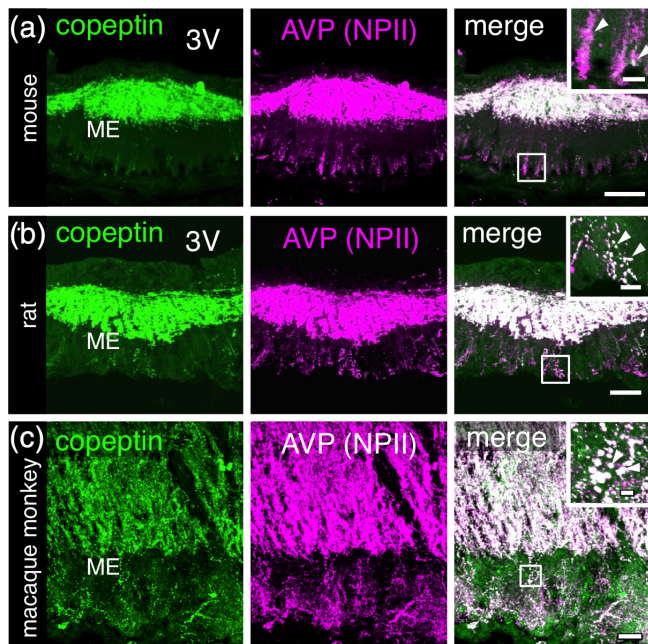


FIGURE 9 Double-label immunofluorescence for N-terminal copeptin and vasopressin (AVP)-neurophysin (NPII) in the median eminence (ME). Representative results are displayed in the mouse (a), in the rat (b), and in the macaque monkey (c). Immunoreactivity against copeptin (green) and AVP (NPII) (magenta) was merged in each right panel (overlap white), respectively. The outlined areas in merged images are enlarged at the top right of the figure. Arrowheads indicate fibers doubly immunopositive for copeptin and AVP (NPII). Scale bars, 50 μm , and 5 μm in enlarged images. 3V, third ventricle [Color figure can be viewed at wileyonlinelibrary.com]

neurosecretory axons, and co-associated within the neurosecretory vesicles (Figure 17b). The size of these vesicles was ~ 160 nm in diameter, characteristic of those of magnocellular neurons in rodents (Armstrong & Tian, 1991; Pow & Morris, 1989; Satoh et al., 2015). However, in the external layer of the mouse ME, although many NPII⁺ dense-cored vesicles (~ 100 nm in diameter) were present in axon terminals, as reported previously (Shaw, Castel, & Morris, 1987), in most terminals the CP8 antiserum detected little or no copeptin immunoreactivity associated with the vesicles (Figure 17c; white arrows). Many neighboring axons contained dense-cored vesicles that were immunoreactive for neither NPII nor copeptin (Figure 17c; black arrows). In a small proportion of nerve terminals in the external layer of the mouse ME, however, dense-cored vesicles containing both CRF- and NPII-immunoreactivity (Figure 17d; white arrows) were present, as expected.

3.4 | Effects of intracerebroventricular injection of a prohormone convertase inhibitor, D6R on the immunoreactivity for copeptin and NPII in mice

We hypothesized that processing of AVP precursor may differ between neuronal populations. Therefore, D6R was injected

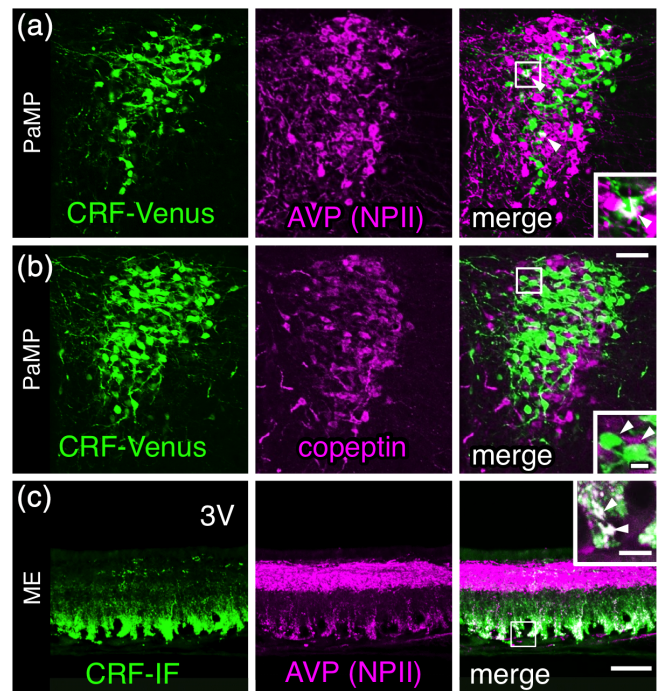


FIGURE 10 Double-label for corticotropin-releasing factor (CRF) and vasopressin (AVP)-neurophysin (NPII) (a) or copeptin (b) in the medial parvocellular part of the paraventricular nucleus (PaMP) of the CRF-Venus Δ Neo mouse. Each outlined area in the merge image is enlarged at the bottom right of the figure. Arrowheads indicate cells doubly immunopositive for CRF-Venus and AVP (NPII) in (a) or single positive for CRF-Venus in (b). (c) In the median eminence (ME) of the wild-type mouse, CRF-immunoreactive fibers were exclusively observed in the external layer, and approximately half of CRF-immunoreactive fibers contained immunodetectable amounts of AVP (NPII) (arrowheads). Many AVP (NPII)-immunoreactive fibers were seen in the internal layer. Scale bars, 50 μm , and 10 μm in enlarged images. IF, immunofluorescence [Color figure can be viewed at wileyonlinelibrary.com]

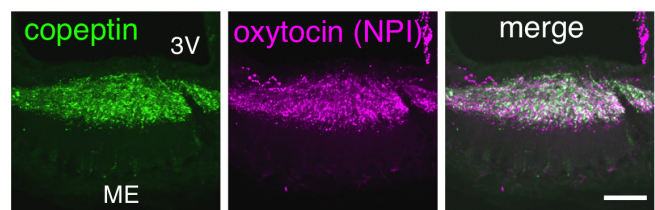


FIGURE 11 Double-label immunofluorescence for copeptin and oxytocin-neurophysin (NPI) in the mouse median eminence (ME). Immunoreactivities against copeptin (green) and NPI (magenta) were merged in the right panel. Scale bar, 50 μm . OC, optic chiasma; 3V, third ventricle [Color figure can be viewed at wileyonlinelibrary.com]

intracerebroventricularly to inhibit the activity of PC1/3, which is a key processing enzyme required for the cleavage of the AVP precursor in the mouse (Figure 18). In the D6R-injected group, many NPII⁺ magnocellular neurons (magenta) exhibited only a faint

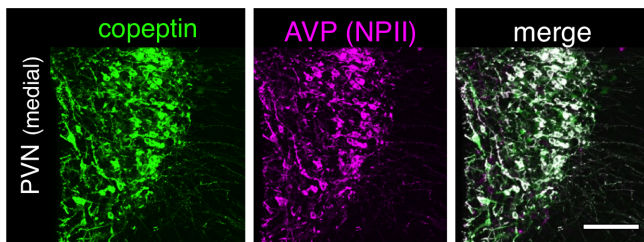


FIGURE 12 Double-label immunofluorescence for copeptin (by using a goat polyclonal antibody against to near the C-terminus of copeptin of mouse origin) and vasopressin-neurophysin (NPII) in the mouse paraventricular nucleus (PVN) (middle part). Immunoreactivities against copeptin (green) and NPII (magenta) were merged in each right panel, respectively. Scale bar, 100 μ m [Color figure can be viewed at wileyonlinelibrary.com]

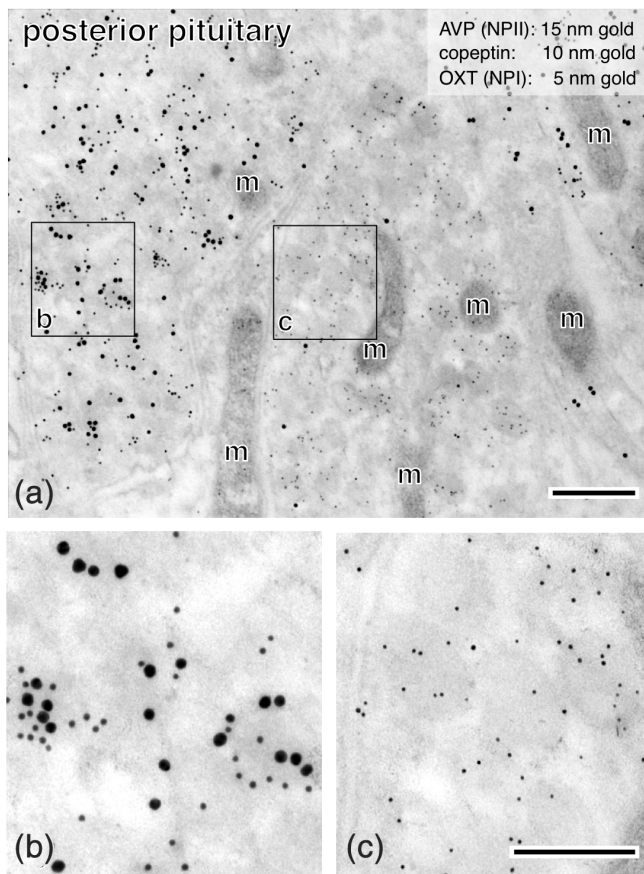


FIGURE 13 Triple immunoelectron microscopy for vasopressin (AVP)-neurophysin (NPII), oxytocin (OXT)-neurophysin (NPI), and N-terminal copeptin in the mouse posterior pituitary. (a) AVP (NPII) (signaled by 15-nm gold particles) and copeptin (signaled by 10-nm gold particles) were both detected within the terminals of magnocellular neurosecretory axons. (b) Enlarged image shows that the immunoreactivity was co-associated with the neurosecretory vesicle structures in the same terminal. (c) In contrast, no copeptin-immunoreactivity was detected in neighboring OXT (NPI)-labeled (by 5-nm gold particles) terminals. Scale bars, 500 nm in (a), and 200 nm in enlarged images (b and c). m, mitochondrion

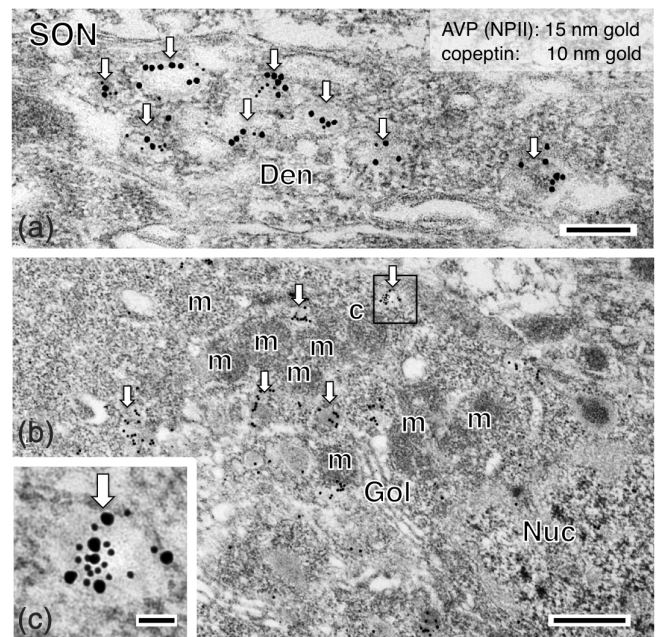


FIGURE 14 Double immunoelectron microscopy for N-terminal copeptin and vasopressin (AVP)-neurophysin (NPII) in the supraoptic nuclei (SON) of the mouse. Numerous neurosecretory vesicles (arrows) located in the dendrites (Den) in (a) and cell bodies of SON neurons in (b) were doubly immunopositive for copeptin (signaled by 10-nm gold particles) and NPII (signaled by 15-nm gold particles). The outlined area in (b) is enlarged in (c). Scale bars, 200 nm in (a), 500 nm in (b), 50 nm in (c). Gol, Golgi apparatus; m, mitochondrion; Nuc, nucleus

immunoreactivity for copeptin (green) in either the PVN or the SON (Figure 18; arrowheads), whereas in the PBS-injected controls most magnocellular NPII⁺ cells exhibited strong copeptin-immunoreactivity (Figure 18). Unexpectedly, several magnocellular neurons that contained copeptin-immunoreactivity but little or no NPII-immunoreactivity were present in the PVN and the SON in the D6R-treated group (Figure 18; arrows in *magno-PVN* and SON). The effect of D6R was also evident in the SCN; NPII⁺ neurons were copeptin-immunoreactive (copeptin⁺/NPII⁺) in the control group (Figure 18), but were almost devoid of copeptin-immunoreactivity in the D6R-treated animals (Figure 18; arrowheads in SCN) (shown in magenta). In the parvocellular PVN, NPII⁺ neurons were mostly copeptin⁻/NPII⁺ (Figure 18; arrowheads in *parvo-PVN*), and neither the number of NPII-immunoreactive neurons nor the copeptin-immunoreactivity in NPII⁺ neurons was affected significantly by D6R treatment (Figure 18; arrowheads in *parvo-PVN*). In the ME, D6R administration had no very obvious effect on the immunostaining for either copeptin or NPII, although NPII-immunoreactivity appeared to decrease a little in the D6R-treated group (Figure 18). Finally, we examined the effect of D6R treatment on AVP peptide immunoreactivity by use of an AVP peptide antiserum. No effect of D6R injection on AVP (mature neuro-peptide) staining was observed (Figure 19).

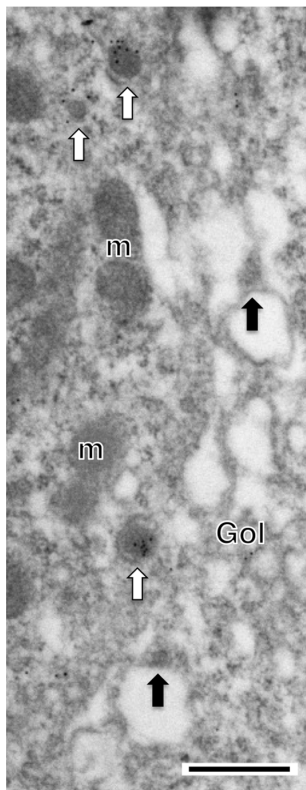


FIGURE 15 Immunoelectron microscopy for copeptin (with the antiserum raised against to near the C-terminus of copeptin of mouse origin: m-20, 10 nm gold particles) in the supraoptic nucleus (SON) of the mouse. Neurosecretory vesicles (arrows) located in the cell bodies of SON neurons were immunopositive for copeptin (signaled by 10-nm gold particles) (white arrows). Copeptin-immunoreactivity was not observed in immature neurosecretory vesicles in the Golgi apparatus (black arrows). Scale bar, 500 nm. Gol, Golgi apparatus; m, mitochondrion

3.5 | Copeptin antisera recognize the processed peptide, but apparently cannot recognize copeptin when it is still part of the prohormone

Finally, we conducted Western blot analysis of the extracts from mouse SON (magnocellular cell body region) and posterior pituitary (terminal region where the precursor processing is complete). The anti-NPII antiserum (PS41), anti-copeptin₇₋₁₄ antiserum (CP8), and Santa Cruz antiserum raised against the C-terminus of mouse copeptin (m-20) were used to examine whether the mature NPII molecule and/or an NPII/copeptin fusion protein molecule could be detected in the respective tissue. We also performed an immunoblotting study for detecting the N-terminus peptide of copeptin with the CP8 antiserum, and for the C-terminus peptide with the m-20 antiserum. A single NPII⁺ band at ~11 kDa was observed in the mouse SON and pituitary (Figure 20). Because the molecular mass of whole copeptin is ~4 kDa, ~15 kDa is the expected total molecular mass of the copeptin and NPII fusion protein. However, a band corresponding to ~15 kDa could not be detected either the CP8

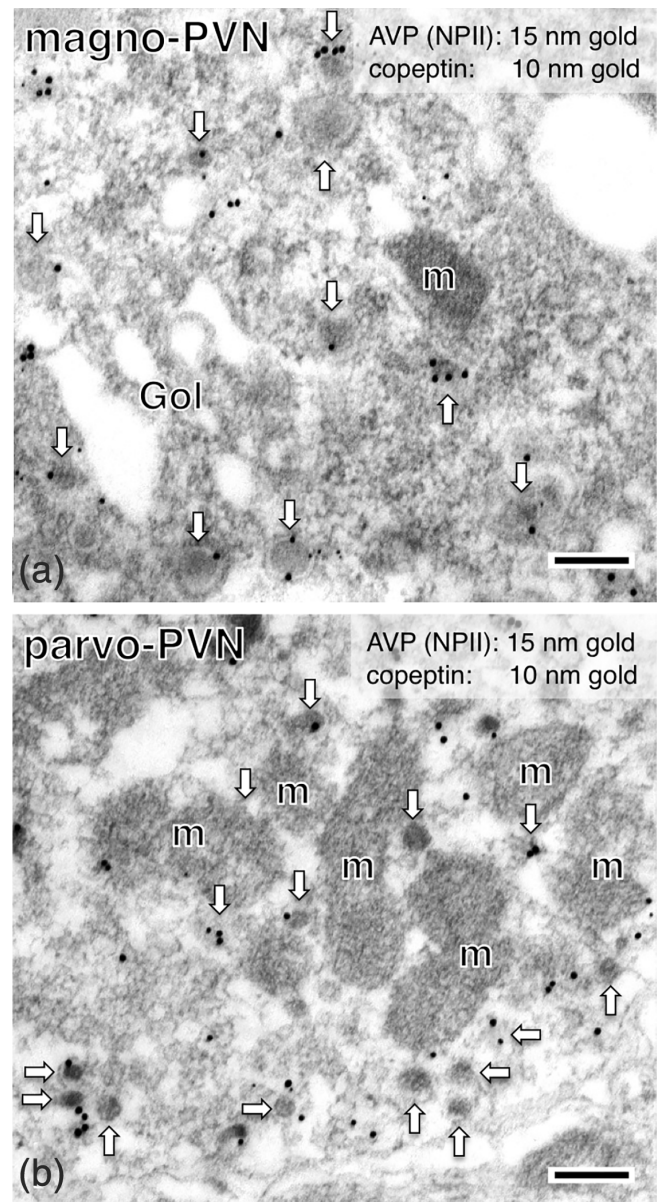


FIGURE 16 Double immunoelectron microscopy for N-terminal copeptin and vasopressin (AVP)-neurophysin (NPII) in the paraventricular nucleus (PVN) of the mouse. (a) In the cell bodies of the magnocellular PVN neurons, numerous neurosecretory vesicles (arrows) were also doubly immunoreactive for copeptin (signaled by 10-nm gold particles) and AVP (NPII) (signaled by 15-nm gold particles). (b) In contrast, although many NPII-immunoreactive dense-core vesicles (signaled by 10-nm gold particles; arrows) were observed in the cell bodies of the parvocellular PVN neurons, they contained essentially no copeptin-immunoreactivity. Scale bars, 200 nm. Gol, Golgi apparatus; m, mitochondrion

(recognizing copeptin₇₋₁₄) or m-20 (recognizing the C-terminus of copeptin) in the extracts from the SON or the pituitary (Figure 20). In addition, our dot blot analysis showed that either of the copeptin antisera (CP8 and m-20) specifically recognize each antigen peptide (Figure 21).

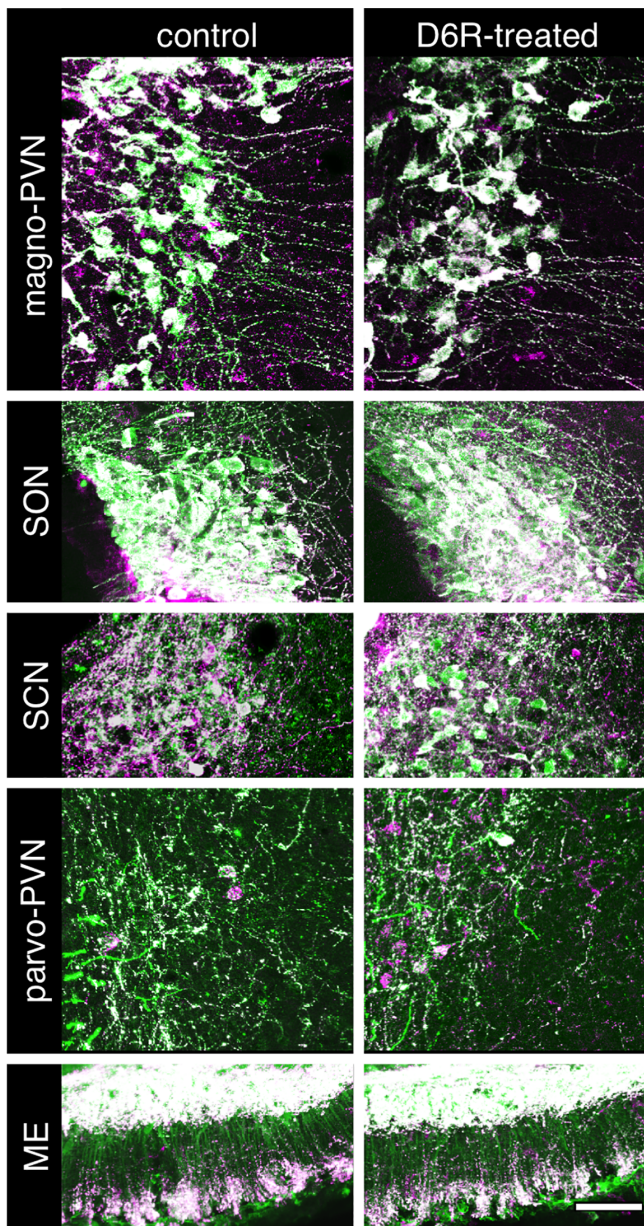


FIGURE 19 Double-label immunofluorescence for vasopressin (AVP) and AVP-neurophysin (NPII) in the magnocellular part of the paraventricular nucleus (*magno-PVN*), the supraoptic nucleus (*SON*), the suprachiasmatic nucleus (*SCN*), the parvocellular part of the PVN (*parvo-PVN*), and the median eminence (*ME*) in the mouse. Representative results are displayed for control tissues (left; *control*) and identical areas after the intracerebroventricular administration of a prohormone convertase inhibitor (hexa-D-arginine amide; D6R) (right; *D6R-treated*). Immunoreactivity against AVP (green) and AVP (NPII) (magenta) was merged in each panel (overlap white). Scale bar, 50 μ m [Color figure can be viewed at wileyonlinelibrary.com]

copeptin⁻/NPII⁺ in the PaAP (~94%) and the posterior parvocellular lateral part (PaPo) (~93%) of the PVN in the mouse. In the rat, copeptin-immunoreactivity could not be identified in approximately half (~53%) of the NPII-immunoreactive neurons in the parvocellular part of the PVN.

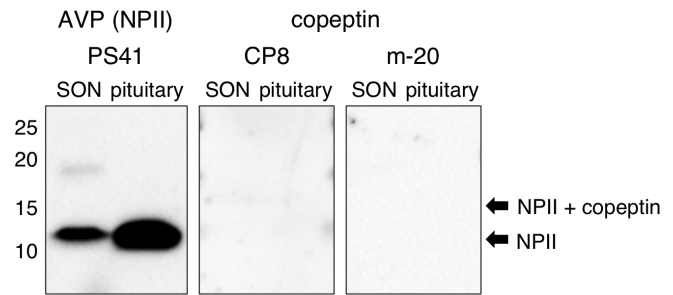


FIGURE 20 Western blot analysis with our custom copeptin₇₋₁₄ (CP8) antiserum, the C-terminus directed Santa Cruz copeptin antiserum (m-20), and a vasopressin (AVP)-neurophysin (NPII) (PS41) monoclonal antibody on similar blots of supraoptic nucleus (SON) and posterior pituitary. A single NPII⁺ band at ~11 kDa was observed in the mouse SON and posterior pituitary. No band could be detected by either of the copeptin antisera at a molecular weight corresponding to a putative NPII/copeptin fusion protein (~15 kDa) in the extracts of either the mouse hypothalamus or pituitary

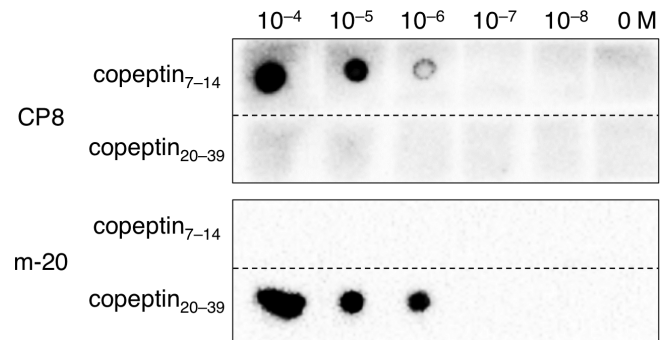


FIGURE 21 Dot blot analysis of antigen peptides probed with our custom copeptin antiserum (CP8) and the antiserum raised against the C-terminus of mouse copeptin (m-20). Each antigen of the mouse origin: copeptin₇₋₁₄ peptide (ATQLDGPA) and copeptin₂₀₋₃₉ (RLVQLAGTRESVDSAKPRVY) were blotted onto the polyvinylidene difluoride membrane (10^{-4} M, 10^{-5} M, 10^{-6} M, 10^{-7} M, 10^{-8} M, and 0 M). Both antibodies recognized each antigen peptide specifically up to $\sim 10^{-6}$ M

The reason(s) for the disproportionately low levels of CP8-immunodetectable copeptin compared with those of NPII and AVP in a substantial proportion of NPII⁺ parvocellular neurons of rats and mice is not clear at present. Proteolytic processing occurs at the dibasic residue lysine-arginine (KR) between the AVP moiety and NPII moiety of the pro-AVP molecule or at the monobasic R site between the NPII moiety and copeptin moiety of the prohormone. Cathepsin L cleaves preferentially the amino terminal of the KR residue, whereas the prohormone convertase family of subtilisin-like proteases (e.g., PC1/3, PC2, PC5) are involved in the cleavage of carboxyl terminals of the KR residue (Hook et al., 2008). Cleavage of the monobasic R site may be catalyzed by a different processing enzyme(s), so pro-AVP processing may take place as a two-step reaction, although a specific enzyme for the monobasic R site cleavage has not yet been

identified. Therefore, one possible explanation for our finding is that the second cleavage between NPII and copeptin does not take place adequately in parvocellular AVP-expressing neurons in rats and mice, possibly through a paucity of a monobasic R protease, and despite the presence of the K/R protease. Indeed, no effect of D6R injection on AVP staining was found in this study, suggesting that a D6R-sensitive enzyme is not involved in the first step of processing (AVP-cleavage and circularization) in mouse AVP neurons. It has been reported that D6R inhibits PC1/3, but does not affect the activity of PC2 (Cameron, Appel, Houghten, & Lindberg, 2000). As yet, for mice, nothing is known of the concentration of the convertases or whether enzymatic activities, such as PC1 and PC2 in parvocellular PVN neurons differ from those of magnocellular AVP neurons. However, for rats, Dong et al. (1997) and Schafer et al. (1993) have both reported that, in the parvocellular PVN neurons, PC2 expression was greater but PC1 expression was much lower than that in the magnocellular PVN and SON neurons. These results suggest that the differential distribution of prohormone convertases between magnocellular and parvocellular PVN subdivisions could play a role in the processing of AVP prohormone in the different cell types. It is possible that, in the rat and mouse, copeptin had been cleaved enzymatically into smaller fragments that were undetectable by our N-terminal custom copeptin antiserum (CP8). Mass spectrometry analysis might, in theory, be able to demonstrate the fragmentation of copeptin in the parvocellular cell bodies. However, the low region-specific resolution of quantitative mass spectrometry at present precludes demonstration of the fragmentation of copeptin in only a subpopulation of parvocellular PVN neurons. Furthermore, our preliminary observation that copeptin could be detected in PVN parvocellular neurons by the m-20 antiserum, which was raised against an epitope close to the C-terminus of mouse copeptin (see Figure 12), shows that the C-terminus at least is intact and available to the antiserum. Our Western blotting experiment using the two copeptin antisera (CP8 and m-20) showed that neither antiserum detected a positive band at a molecular weight (~15 kDa) corresponding to copeptin incorporated as part of the AVP precursor in extracts of either mouse hypothalamus or pituitary. Our dot blot analysis also supports our hypothesis that both copeptin antisera specifically recognize each antigen peptide (Figure 21). In addition, we previously reported by Western blot analysis that our custom copeptin₇₋₁₄ antiserum (CP8) specifically recognizes the copeptin₁₋₁₄ (fragment)-GFP fusion protein (Satoh et al., 2015). Furthermore, our post-embedding immunoelectron microscopy showed that immunoreactivity to our custom copeptin₇₋₁₄ antiserum (CP8), the Santa Cruz copeptin polyclonal antiserum (m-20), and the anti-NPII monoclonal antibody (PS41) could all be detected in neurosecretory vesicles within magnocellular AVP neurons, but apparently not in immature vesicle cores within the Golgi apparatus. Taken together, these results indicate that both copeptin antisera used in this study recognize only the processed peptide, and do not recognize copeptin when it is still part of a prohormone. In sharp contrast to the lack of copeptin-immunoreactivity in most NPII⁺ parvocellular neurons in the rodent PVN, most parvocellular PVN NPII⁺ neurons in the monkey exhibited prominent copeptin-immunoreactivity, demonstrating a

striking species difference in copeptin expression between rodents and the monkey in NPII-immunoreactive CRF parvocellular neurons in the PVN. Taken together, these results suggest that there is a difference between magnocellular and parvocellular neurons in the proteolytic processing of the AVP precursor in rodents, but it remains unclear whether this is simply a difference in the speed of processing, and what might be its functional import.

Glycosylation of copeptin increases the stability of the peptide and its plasma half-life (Bhandari et al., 2009; Blanchard et al., 2013; Bolignano et al., 2014; Wuttke et al., 2013). Therefore, a third possible explanation for the relative lack of CP8-detectable copeptin in rodent parvocellular neurons would be that the glycosylation has not been completed in these neurons, leading to rapid breakdown of copeptin. Our preliminary finding that the copeptin is, however, detectable with the m-20 C-terminal antiserum makes this possibility unlikely.

It has long been known that a subset of CRF neurons in the PVN co-expresses AVP in rats (Whitnall et al., 1985), mice (Whitnall, 1993), and humans (Mouri et al., 1993; Whitnall, 1993). CRF and AVP are co-secreted from nerve endings in the ME into capillaries, and reach the anterior pituitary via portal vessels to stimulate synergistically the release of ACTH from corticotrophs (Jones & Gillham, 1988). It is currently unclear whether only a subset of CRF neurons is capable of expressing AVP, or whether the transcription of the AVP gene and/or the subsequent production of AVP peptide are dependent on neural and humoral factors influencing the activity of the cell. Although very few parvocellular neurons are immunopositive for both CRF and AVP in unstressed mice, exposure to stress (Whitnall, 1993) or adrenalectomy (Itoi et al., 2014) increases dramatically the number of doubly immunopositive cells. In the external layer of the ME, about half of the parvocellular CRF nerve endings contain detectable AVP in the rat (Whitnall, 1993; Whitnall et al., 1985), whereas in the mouse virtually all CRF neurosecretory axons in the external layer of the ME contain AVP (Whitnall, 1993). In humans, AVP can be detected in all CRF neurons, depending on the premortem conditions (Mouri et al., 1993). In the present study, very few CRF⁺ neurons in the PVN of the *CRF-VenusΔNeo* mouse exhibited N-terminal copeptin-immunoreactivity, at least under normal unstressed circadian glucocorticoid levels, a finding consistent with an idea that AVP expression in CRF neurons is sensitive to stress and circulating glucocorticoid concentrations (Itoi et al., 2014). Another subpopulation of CRF⁺ and/or AVP⁺ parvocellular PVN neurons is known to project to autonomic centers in the brainstem and spinal cord, and it is likely that these neurons are unresponsive to negative feedback by glucocorticoids (Sawchenko, 1987). The copeptin status of this subpopulation of neurons remains to be determined.

In the mouse, very little copeptin-immunoreactivity could be identified in nerve terminals of parvocellular CRF neurons at the external layer of the ME with the N-terminal CP8 antiserum, and the reason for this remains unclear. It is reported that, in the ox, copeptin (39aa: 1–39) is metabolized into several small peptides of 10aa (1–10), 18aa (1–18), 17aa (23–39), and 14aa (26–39) residues (Land et al., 1982; Smyth & Massey, 1979). If copeptin in the mouse parvocellular neurons is metabolized rapidly, then this could explain

why it was undetectable in most, but not all, nerve fibers in the external ME with the CP8 antiserum. In particular, peptides produced by enzymatic cleavage between ¹⁰[L] and ¹¹[D] may not be identified because our custom CP8 copeptin antiserum was raised against an epitope that encompasses amino acid residues ⁷[A] to ¹⁴[A]. However, copeptin-immunoreactivity was readily detectable with the CP8 antiserum in some NPII-expressing nerve endings at the external layer of the ME in the rat and the monkey, reiterating the species difference in copeptin-immunoreactivity. Furthermore, our preliminary study shows that the m-20 C-terminal antiserum can detect copeptin immunoreactivity in both the cell bodies and the terminals of parvocellular NPII⁺ neurons of mice (Figure 12), which indicates that the C-terminal epitope has not been metabolized to the extent that it is unrecognizable. Interpretation of any apparent differences in immunocytochemical detection of parvocellular neuropeptides between the cell bodies and terminals is difficult because of the concentration of the neurosecretory vesicles in the axon terminals (Morris, 2020). However, relatively slow processing of the pro-AVP precursor could explain why copeptin-immunoreactivity in the ME was more intense than that in the parvocellular PVN perikarya. Although AVP neurons in the SCN are also small-sized neurons, virtually all NPII⁺ SCN neurons were copeptin⁺/NPII⁺ in both mice and rats. Thus, SCN neurons resemble magnocellular neurons in terms of the N-terminal (CP8) copeptin-immunoreactivity.

Intracerebroventricular administration of a prohormone convertase inhibitor, D6R, resulted in a marked reduction of copeptin-immunoreactivity in the NPII-immunoreactive magnocellular PVN neurons and in SCN neurons in the mice. This result raises the possibility that insufficient processing of the prohormone could explain the lack of N-terminal copeptin immunoreactivity in a subpopulation of NPII (AVP)-expressing parvocellular neurons. Indeed, the second cleavage (between NPII and copeptin residues) is incomplete in birds and amphibians, and a two-domain protein comprising NPII and copeptin has been identified as a "big NP" in the posterior pituitary and in the circulation (Acher, 1980; Michel, Chauvet, Chauvet, & Acher, 1987). The absence of S–S bonds in the "big NP" is likely to have resulted in an alteration in three-dimensional structure and could provide another explanation for the lower NPII (PS41) immunostaining of magnocellular neurosecretory neurons in the D6R-treated animals. As mentioned above, our Western blot evidence (Figure 20) indicates that neither the N-terminal (CP8) nor the C-terminal (m-20) copeptin antisera used in this study recognize any precursor protein like "big NP" in extracts of the SON or posterior pituitary. In addition, D6R is known to be predominantly a furin inhibitor (Cameron et al., 2000), and both Schafer et al. (1993) and Dong et al. (1997) reported the ubiquitous presence of furin in the PVN and SON.

Copeptin has long been regarded as biologically inactive (Morgenthaler et al., 2008). However, recent advances in research on the glycopeptide mean that it is now widely accepted that copeptin possesses multi-faceted biological properties. For example, copeptin is required for correct folding of the AVP precursor, and its absence may lead to an inefficient monomer folding that contributes

to the pathogenesis of human hypothalamic diabetes insipidus (Barat, Simpson, & Breslow, 2004). Roles of copeptin in modulating cellular functions have also been explored, and it has been reported that copeptin causes a low amplitude, slow increase of [Ca²⁺]_i in a population of cultured rat hypothalamic neurons (Gao et al., 2008). Copeptin (both copeptin 1–39 [full length] and the C-terminal fragment 22–39) also potentiates the amplitude of excitatory postsynaptic potentials evoked in neurons of the rat lateral septum (van den Hooff, Seger, Burbach, & Urban, 1990), indicating that the C-terminal component of copeptin may modulate neuronal activity in the brain.

In conclusion, N-terminal copeptin-immunoreactivity was not detectable (or was present in disproportionately low concentrations) in a subpopulation of AVP-expressing parvocellular neurons in the PVN of rodents, but was present in virtually all AVP-expressing magnocellular neurons in the PVN and SON. This difference between parvocellular and magnocellular copeptin expression was not observed in the monkey, and was not seen when the copeptin was detected with a C-terminal copeptin antiserum. This study has revealed not only that there are species differences in the processing of the pro-AVP precursor and production of free copeptin, but also that the processing may not be the same in different groups of pro-AVP-expressing cells within a given species. At the moment, there is an increasing use of plasma copeptin measurements as a surrogate marker for AVP measurements in human clinical problems such as diabetes insipidus, sepsis and cardiovascular disease (Morgenthaler et al., 2008). Future research on macaques could provide valuable and relevant information on copeptin processing and plasma copeptin levels under conditions such as dehydration and other stresses. However, relatively little is currently known about the control of pro-AVP precursor processing in humans, the enzymes involved, and the extent to which the various antibodies used to detect copeptin recognize the possible different molecular weight forms. Our results, which reveal for the first time differences among rodents and macaques, strongly suggest that this is an area which deserves further experimental exploration.

ACKNOWLEDGMENTS

The authors thank Prof Mitsuhiro Kawata, Prof Minoru Kimura, Prof Kazuhiro Yagita (Kyoto Prefectural University of Medicine, Japan), Prof Masaki Isoda (National Institute for Physiological Sciences, Japan), and Prof Kae Nakamura (Kansai Medical University, Japan) for providing the macaque monkey tissues, their encouragement, and/or critical discussion of this study. Tissues of Nihonzaru (Japanese macaque monkeys) were provided by National Institutes of Natural Sciences (NINS) through the National Bio-Resource Project (NBRP) "Nihonzaru" of the MEXT, Japan. This work was supported by the Japan Society for the Promotion of Science (JSPS) KAKENHI (to H. S.; 15K15202, 15KK0257, 15H05724, 16H06280 (ABIS); to K. T.; 15J40220, 19K06475; to K.I. 18K08499; to S. M.; 20K06722; to T. O.; 13J08283, 20K15837; to K. S.; 16J06859) and from the Japan Agency for Medical Research and Development (AMED) (to H. S.; 961149). K. S., T. O., and K. T. were supported by Research Fellowships of JSPS for Young Scientists.

CONFLICT OF INTEREST

The authors declare no conflict of interest.

AUTHOR CONTRIBUTIONS

Natsuko Kawakami, Akito Otubo, Keita Satoh, Sho Maejima, Ashraf H. Talukder, Yasumasa Ueda, Takumi Oti, Keiko Takanami, Keiichi Itoi, and Hirotaka Sakamoto performed immunohistochemical experiments. **Natsuko Kawakami, John F. Morris, and Hirotaka Sakamoto** performed immunoelectron microscopy analyses. **Keiichi Itoi, John F. Morris, and Tatsuya Sakamoto** interpreted the data and provided mutant mice, advice, and equipment. **Hirotaka Sakamoto** wrote the paper with assistance from **Keiichi Itoi** and **John F. Morris**. **Natsuko Kawakami** and **Akito Otubo** contributed equally to this study. **Hirotaka Sakamoto** supervised the whole study. All authors had full access to all the data in the study and take responsibility for the integrity of the data and the accuracy of the data analysis.

PEER REVIEW

The peer review history for this article is available at <https://publons.com/publon/10.1002/cne.25026>.

DATA AVAILABILITY STATEMENT

There is no supplementary material of this article.

ORCID

Hirotaka Sakamoto  <https://orcid.org/0000-0002-6224-4591>

REFERENCES

- Acher, R. (1980). Molecular evolution of biologically active polypeptides. *Proceedings of the Royal Society of London - Series B: Biological Sciences*, 210(1178), 21–43.
- Armstrong, W. E., & Tian, M. (1991). Separate ultrastructural distributions of neurophysin and C-terminal glycopeptide within dense core vesicles in rat neural lobe. *Brain Research*, 562(1), 144–148. [https://doi.org/10.1016/0006-8993\(91\)91198-a](https://doi.org/10.1016/0006-8993(91)91198-a)
- Barat, C., Simpson, L., & Breslow, E. (2004). Properties of human vasopressin precursor constructs: Inefficient monomer folding in the absence of copeptin as a potential contributor to diabetes insipidus. *Biochemistry*, 43(25), 8191–8203. <https://doi.org/10.1021/bi0400094>
- Ben-Barak, Y., Russell, J. T., Whitnall, M. H., Ozato, K., & Gainer, H. (1985). Neurophysin in the hypothalamo-neurohypophysial system. I. Production and characterization of monoclonal antibodies. *The Journal of Neuroscience*, 5(1), 81–97.
- Bhandari, S. S., Loke, I., Davies, J. E., Squire, I. B., Struck, J., & Ng, L. L. (2009). Gender and renal function influence plasma levels of copeptin in healthy individuals. *Clinical Science (London, England)*, 116(3), 257–263. <https://doi.org/10.1042/CS20080140CS20080140>
- Biag, J., Huang, Y., Gou, L., Hintiryan, H., Askarinam, A., Hahn, J. D., ... Dong, H. W. (2012). Cyto- and chemoarchitecture of the hypothalamic paraventricular nucleus in the C57BL/6J male mouse: A study of immunostaining and multiple fluorescent tract tracing. *The Journal of Comparative Neurology*, 520(1), 6–33. <https://doi.org/10.1002/cne.22698>
- Blanchard, A., Steichen, O., de Mota, N., Curis, E., Gauci, C., Frank, M., ... Llorens-Cortes, C. (2013). An abnormal apelin/vasopressin balance may contribute to water retention in patients with the syndrome of inappropriate antidiuretic hormone (SIADH) and heart failure. *The Journal of Clinical Endocrinology and Metabolism*, 98(5), 2084–2089. <https://doi.org/10.1210/jc.2012-3794jc.2012-3794>
- Bolignano, D., Cabassi, A., Fiaccadori, E., Ghigo, E., Pasquali, R., Peracino, A., ... Zoccali, C. (2014). Copeptin (CTproAVP), a new tool for understanding the role of vasopressin in pathophysiology. *Clinical Chemistry and Laboratory Medicine*, 52, 1447–1456. <https://doi.org/10.1515/cclm-2014-0379/j/cclm.ahead-of-print/cclm-2014-0379/cclm-2014-0379.xml>
- Breslow, E. (1993). Structure and folding properties of neurophysin and its peptide complexes: Biological implications. *Regulatory Peptides*, 45(1–2), 15–19.
- Burbach, J. P., Luckman, S. M., Murphy, D., & Gainer, H. (2001). Gene regulation in the magnocellular hypothalamo-neurohypophysial system. *Physiological Reviews*, 81(3), 1197–1267. <https://doi.org/10.1152/physrev.2001.81.3.1197>
- Cameron, A., Appel, J., Houghten, R. A., & Lindberg, I. (2000). Polyarginines are potent furin inhibitors. *The Journal of Biological Chemistry*, 275(47), 36741–36749. <https://doi.org/10.1074/jbc.M003848200>
- Castel, M., & Morris, J. F. (1988). The neurophysin-containing innervation of the forebrain of the mouse. *Neuroscience*, 24(3), 937–966. [https://doi.org/10.1016/0306-4522\(88\)90078-4](https://doi.org/10.1016/0306-4522(88)90078-4)
- Castel, M., Morris, J. F., Whitnall, M. H., & Sivan, N. (1986). Improved visualization of the immunoreactive hypothalamo-neurohypophysial system by use of immuno-gold techniques. *Cell and Tissue Research*, 243(1), 193–204.
- Davies, J., Waller, S., Zeng, Q., Wells, S., & Murphy, D. (2003). Further delineation of the sequences required for the expression and physiological regulation of the vasopressin gene in transgenic rat hypothalamic magnocellular neurones. *Journal of Neuroendocrinology*, 15(1), 42–50 doi:865.
- de Goeij, D. C., Jezova, D., & Tilders, F. J. (1992). Repeated stress enhances vasopressin synthesis in corticotropin releasing factor neurons in the paraventricular nucleus. *Brain Research*, 577(1), 165–168. [https://doi.org/10.1016/0006-8993\(92\)90552-k](https://doi.org/10.1016/0006-8993(92)90552-k)
- Dong, W., Seidel, B., Marcinkiewicz, M., Chretien, M., Seidah, N. G., & Day, R. (1997). Cellular localization of the prohormone convertases in the hypothalamic paraventricular and supraoptic nuclei: Selective regulation of PC1 in corticotrophin-releasing hormone parvocellular neurons mediated by glucocorticoids. *The Journal of Neuroscience*, 17(2), 563–575.
- Fellmann, D., Bugnon, C., Bresson, J. L., Gouget, A., Cardot, J., Clavequin, M. C., & Hadjiyiassemis, M. (1984). The CRF neuron: Immunocytochemical study. *Peptides*, 5(Suppl 1), 19–33.
- Fischman, A. J., & Moldow, R. L. (1984). In vivo potentiation of corticotropin releasing factor activity by vasopressin analogues. *Life Sciences*, 35(12), 1311–1319. [https://doi.org/10.1016/0024-3205\(84\)90103-6](https://doi.org/10.1016/0024-3205(84)90103-6)
- Franklin, K. B. J., & Paxinos, G. (2007). *The mouse brain in stereotaxic coordinates* (3rd ed.). Amsterdam: Elsevier.
- Gao, X., Brailoiu, G. C., Brailoiu, E., Dun, S. L., Yang, J., Chang, J. K., & Dun, N. J. (2008). Copeptin immunoreactivity and calcium mobilisation in hypothalamic neurones of the rat. *Journal of Neuroendocrinology*, 20(11), 1242–1251. <https://doi.org/10.1111/j.1365-2826.2008.01782.x>
- Gillies, G. E., Linton, E. A., & Lowry, P. J. (1982). Corticotropin releasing activity of the new CRF is potentiated several times by vasopressin. *Nature*, 299(5881), 355–357. <https://doi.org/10.1038/299355a0>
- Gizowski, C., Zaelzer, C., & Bourque, C. W. (2016). Clock-driven vasopressin neurotransmission mediates anticipatory thirst prior to sleep. *Nature*, 537(7622), 685–688. <https://doi.org/10.1038/nature19756>
- Golombek, D. A., & Rosenstein, R. E. (2010). Physiology of circadian entrainment. *Physiological Reviews*, 90(3), 1063–1102. <https://doi.org/10.1152/physrev.00009.2009>
- Hashimoto, K., Murakami, K., Hattori, T., & Ota, Z. (1984). Synergistic interaction of corticotropin releasing factor and arginine vasopressin on adrenocorticotropin and cortisol secretion in *Macaca fuscata*. *Acta*

- Medica Okayama*, 38(3), 261–267. <https://doi.org/10.18926/AMO/30349>
- Hook, V., Funkelstein, L., Lu, D., Bark, S., Wegrzyn, J., & Hwang, S. R. (2008). Proteases for processing proneuropeptides into peptide neurotransmitters and hormones. *Annual Review of Pharmacology and Toxicology*, 48, 393–423. <https://doi.org/10.1146/annurev.pharmtox.48.113006.094812>
- Itoi, K., Talukder, A. H., Fuse, T., Kaneko, T., Ozawa, R., Sato, T., ... Sakimura, K. (2014). Visualization of corticotropin-releasing factor neurons by fluorescent proteins in the mouse brain and characterization of labeled neurons in the paraventricular nucleus of the hypothalamus. *Endocrinology*, 155(10), 4054–4060. <https://doi.org/10.1210/en.2014-1182>
- Johnson, Z. V., & Young, L. J. (2017). Oxytocin and vasopressin neural networks: Implications for social behavioral diversity and translational neuroscience. *Neuroscience & Biobehavioral Reviews*, 76(Pt A), 87–98. <https://doi.org/10.1016/j.neubiorev.2017.01.034>
- Jones, M. T., & Gillham, B. (1988). Factors involved in the regulation of adrenocorticotrophic hormone/beta-lipotrophic hormone. *Physiological Reviews*, 68(3), 743–818. <https://doi.org/10.1152/physrev.1988.68.3.743>
- Kono, J., Konno, K., Talukder, A. H., Fuse, T., Abe, M., Uchida, K., ... Itoi, K. (2017). Distribution of corticotropin-releasing factor neurons in the mouse brain: A study using corticotropin-releasing factor-modified yellow fluorescent protein knock-in mouse. *Brain Structure & Function*, 222(4), 1705–1732. <https://doi.org/10.1007/s00429-016-1303-0>
- Koshimizu, T. A., Nakamura, K., Egashira, N., Hiroyama, M., Nonoguchi, H., & Tanoue, A. (2012). Vasopressin V1a and V1b receptors: From molecules to physiological systems. *Physiological Reviews*, 92(4), 1813–1864. <https://doi.org/10.1152/physrev.00035.2011>
- Land, H., Schutz, G., Schmale, H., & Richter, D. (1982). Nucleotide sequence of cloned cDNA encoding bovine arginine vasopressin-neurophysin II precursor. *Nature*, 295(5847), 299–303.
- Liu, J. H., Muse, K., Contreras, P., Gibbs, D., Vale, W., Rivier, J., & Yen, S. S. (1983). Augmentation of ACTH-releasing activity of synthetic corticotropin releasing factor (CRF) by vasopressin in women. *The Journal of Clinical Endocrinology and Metabolism*, 57(5), 1087–1089. <https://doi.org/10.1210/jcem-57-5-1087>
- Ludwig, M., & Leng, G. (2006). Dendritic peptide release and peptide-dependent behaviours. *Nature Reviews. Neuroscience*, 7(2), 126–136.
- Michel, G., Chauvet, J., Chauvet, M. T., & Acher, R. (1987). One-step processing of the amphibian vasotocin precursor: Structure of a frog (*Rana esculenta*) "big" neurophysin. *Biochemical and Biophysical Research Communications*, 149(2), 538–544.
- Morgenthaler, N. G., Struck, J., Jochberger, S., & Dunser, M. W. (2008). Copeptin: Clinical use of a new biomarker. *Trends in Endocrinology and Metabolism*, 19(2), 43–49. <https://doi.org/10.1016/j.tem.2007.11.001>
- Morris, J. (2020). Neurosecretory vesicles: Structure, distribution, release and breakdown. In G. Lemons & J. R. Dayanithi (Eds.), *Neurosecretion: Secretory mechanisms* (Vol. 8, pp. 81–102). Switzerland: Springer Nature.
- Mouri, T., Itoi, K., Takahashi, K., Suda, T., Murakami, O., Yoshinaga, K., ... Sasano, N. (1993). Colocalization of corticotropin-releasing factor and vasopressin in the paraventricular nucleus of the human hypothalamus. *Neuroendocrinology*, 57(1), 34–39. <https://doi.org/10.1159/000126339>
- Murakami, K., Hashimoto, K., & Ota, Z. (1984). Interaction of synthetic ovine corticotropin releasing factor and arginine vasopressin on in vitro ACTH release by the anterior pituitary of rats. *Neuroendocrinology*, 39(1), 49–53. <https://doi.org/10.1159/000123954>
- Murphy, D., Waller, S., Fairhall, K., Carter, D. A., & Robinson, C. A. (1998). Regulation of the synthesis and secretion of vasopressin. *Progress in Brain Research*, 119, 137–143. [https://doi.org/10.1016/s0079-6123\(08\)61567-8](https://doi.org/10.1016/s0079-6123(08)61567-8)
- Otero-Garcia, M., Martin-Sanchez, A., Fortes-Marco, L., Martinez-Ricos, J., Agustin-Pavon, C., Lanuza, E., & Martinez-Garcia, F. (2014). Extending the socio-sexual brain: Arginine-vasopressin immunoreactive circuits in the telencephalon of mice. *Brain Structure & Function*, 219(3), 1055–1081. <https://doi.org/10.1007/s00429-013-0553-3>
- Plotsky, P. M. (1987). Regulation of hypophysiotropic factors mediating ACTH secretion. *Annals of the New York Academy of Sciences*, 512, 205–217. <https://doi.org/10.1111/j.1749-6632.1987.tb24962.x>
- Plotsky, P. M., & Sawchenko, P. E. (1987). Hypophysial-portal plasma levels, median eminence content, and immunohistochemical staining of corticotropin-releasing factor, arginine vasopressin, and oxytocin after pharmacological adrenalectomy. *Endocrinology*, 120(4), 1361–1369. <https://doi.org/10.1210/endo-120-4-1361>
- Pow, D. V., & Morris, J. F. (1989). Dendrites of hypothalamic magnocellular neurons release neurohypophysial peptides by exocytosis. *Neuroscience*, 32(2), 435–439.
- Ramkisoensing, A., & Meijer, J. H. (2015). Synchronization of biological clock neurons by light and peripheral feedback systems promotes circadian rhythms and health. *Frontiers in Neurology*, 6, 128. <https://doi.org/10.3389/fneur.2015.00128>
- Rivier, C., & Vale, W. (1983). Interaction of corticotropin-releasing factor and arginine vasopressin on adrenocorticotropin secretion in vivo. *Endocrinology*, 113(3), 939–942. <https://doi.org/10.1210/endo-113-3-939>
- Sakamoto, H., Matsuda, K.-I., Zuloaga, D. G., Hongu, H., Wada, E., Wada, K., ... Kawata, M. (2008). Sexually dimorphic gastrin releasing peptide system in the spinal cord controls male reproductive functions. *Nature Neuroscience*, 11(6), 634–636.
- Satoh, K., Oti, T., Katoh, A., Ueta, Y., Morris, J. F., Sakamoto, T., & Sakamoto, H. (2015). In vivo processing and release into the circulation of GFP fusion protein in arginine vasopressin enhanced GFP transgenic rats: Response to osmotic stimulation. *The FEBS Journal*, 282(13), 2488–2499. <https://doi.org/10.1111/febs.13291>
- Sawchenko, P. E. (1987). Evidence for differential regulation of corticotropin-releasing factor and vasopressin immunoreactivities in parvocellular neurosecretory and autonomic-related projections of the paraventricular nucleus. *Brain Research*, 437(2), 253–263. [https://doi.org/10.1016/0006-8993\(87\)91641-6](https://doi.org/10.1016/0006-8993(87)91641-6)
- Sawchenko, P. E., Arias, C. A., & Mortrud, M. T. (1993). Local tetrodotoxin blocks chronic stress effects on corticotropin-releasing factor and vasopressin messenger ribonucleic acids in hypophysiotropic neurons. *Journal of Neuroendocrinology*, 5(4), 341–348. <https://doi.org/10.1111/j.1365-2826.1993.tb00493.x>
- Sawchenko, P. E., Swanson, L. W., & Vale, W. W. (1984). Co-expression of corticotropin-releasing factor and vasopressin immunoreactivity in parvocellular neurosecretory neurons of the adrenalectomized rat. *Proceedings of the National Academy of Sciences of the United States of America*, 81(6), 1883–1887.
- Schafer, M. K., Day, R., Cullinan, W. E., Chretien, M., Seidah, N. G., & Watson, S. J. (1993). Gene expression of prohormone and proprotein convertases in the rat CNS: A comparative in situ hybridization analysis. *The Journal of Neuroscience*, 13(3), 1258–1279.
- Shaw, F. D., Castel, M., & Morris, J. F. (1987). Ultrastructural characterization of vasopressinergic terminals in the lateral septum of murine brains by use of monoclonal anti-neurophysins. *Cell and Tissue Research*, 249(2), 403–410.
- Smyth, D. G., & Massey, D. E. (1979). A new glycopeptide in pig, ox and sheep pituitary. *Biochemical and Biophysical Research Communications*, 87(4), 1006–1010. [https://doi.org/10.1016/s0006-291x\(79\)80007-8](https://doi.org/10.1016/s0006-291x(79)80007-8)
- Trudel, E., & Bourque, C. W. (2010). Central clock excites vasopressin neurons by waking osmosensory afferents during late sleep. *Nature Neuroscience*, 13(4), 467–474. <https://doi.org/10.1038/nn.2503>
- Vale, W., Vaughan, J., Smith, M., Yamamoto, G., Rivier, J., & Rivier, C. (1983). Effects of synthetic ovine corticotropin-releasing factor, glucocorticoids, catecholamines, neurohypophysial peptides, and other substances on cultured corticotropic cells. *Endocrinology*, 113(3), 1121–1131. <https://doi.org/10.1210/endo-113-3-1121>

- van den Hooff, P., Seger, M. A., Burbach, J. P., & Urban, I. J. (1990). The C-terminal glycopeptide of propressophysin potentiates excitatory transmission in the rat lateral septum. *Neuroscience*, *37*(3), 647–653.
- Wang, H., Ward, A. R., & Morris, J. F. (1995). Oestradiol acutely stimulates exocytosis of oxytocin and vasopressin from dendrites and somata of hypothalamic magnocellular neurons. *Neuroscience*, *68*(4), 1179–1188. [https://doi.org/10.1016/0306-4522\(95\)00186-M](https://doi.org/10.1016/0306-4522(95)00186-M)
- Whitnall, M. H. (1993). Regulation of the hypothalamic corticotropin-releasing hormone neurosecretory system. *Progress in Neurobiology*, *40*(5), 573–629.
- Whitnall, M. H., Mezey, E., & Gainer, H. (1985). Co-localization of corticotropin-releasing factor and vasopressin in median eminence neurosecretory vesicles. *Nature*, *317*(6034), 248–250.
- Wuttke, A., Dixit, K. C., Szinnai, G., Werth, S. C., Haagen, U., Christ-Crain, M., ... Brabant, G. (2013). Copeptin as a marker for

arginine-vasopressin/antidiuretic hormone secretion in the diagnosis of paraneoplastic syndrome of inappropriate ADH secretion. *Endocrine*, *44*(3), 744–749. <https://doi.org/10.1007/s12020-013-9919-9>

How to cite this article: Kawakami N, Otubo A, Maejima S, et al. Variation of pro-vasopressin processing in parvocellular and magnocellular neurons in the paraventricular nucleus of the hypothalamus: Evidence from the vasopressin-related glycopeptide copeptin. *J Comp Neurol*. 2020;1–19. <https://doi.org/10.1002/cne.25026>